

Signals of Success and Struggle: Early Prediction and Physiological Signatures of Human Performance across Task Complexity

Yufei Cao

School of Computing
The Australian National University
Canberra, ACT, Australia
yufei.cao1@anu.edu.au

Ziyu Chen

Computational Media Lab
The Australian National University
Canberra, ACT, Australia
ziyu.chen@anu.edu.au

Penny Sweetser

School of Computing
The Australian National University
Canberra, ACT, Australia
penny.kyburz@anu.edu.au

Xuanying Zhu

The Australian National University
Canberra, ACT, Australia
xuanying.zhu@anu.edu.au

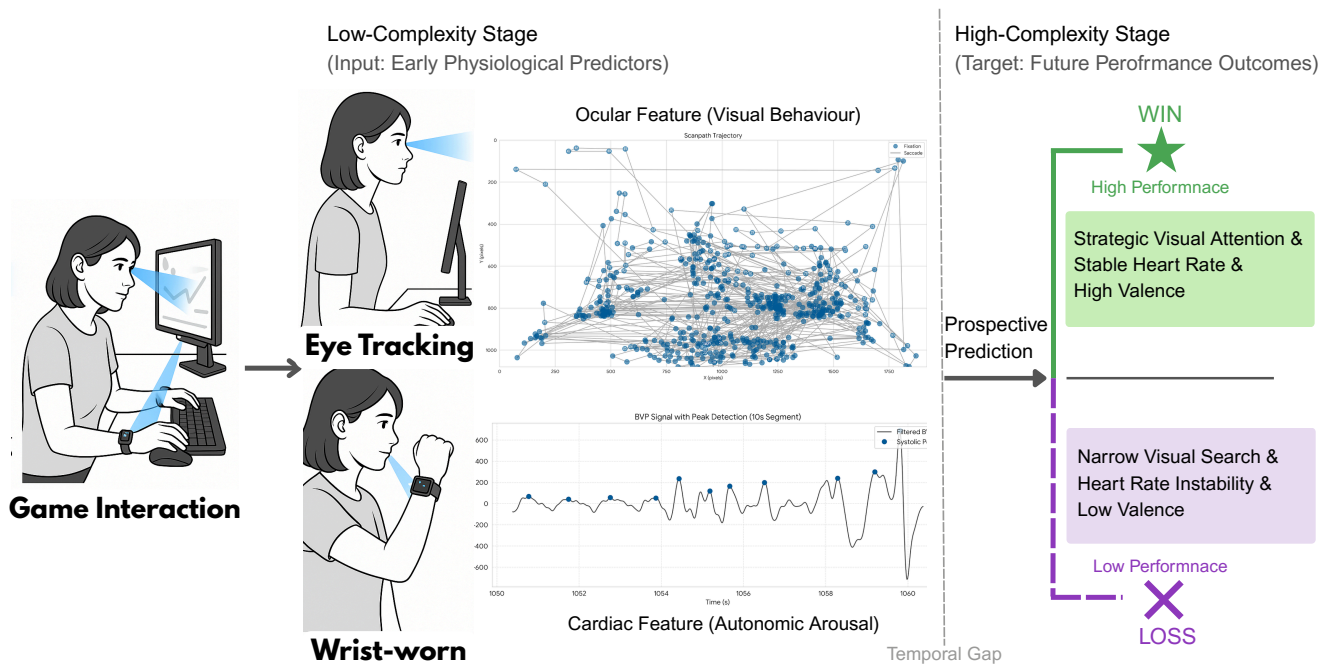


Figure 1: Overview of the prospective prediction pipeline. Early ocular and cardiac features from the low-complexity game session are used to predict performance outcomes in the subsequent high-complexity session. Ocular features capture visual behaviour, while cardiac features reflect autonomic arousal. Differences in visual patterns, autonomic profiles, and affective states are observed between high- and low-performing groups.

Abstract

User performance is crucial in interactive systems, capturing how effectively users engage with task execution. Prospectively predicting

performance enables the timely identification of users struggling with task demands. While ocular and cardiac signals are widely used to characterise performance-relevant visual behaviour and physiological activation, their potential for early prediction and for revealing the physiological mechanisms underlying performance differences remains underexplored. We conducted a within-subject experiment in a game environment with naturally unfolding complexity, using early ocular and cardiac signals to predict later performance and to examine physiological and self-reported group differences. Results show that the ocular-cardiac fusion model



This work is licensed under a Creative Commons Attribution 4.0 International License.
CHI '26, Barcelona, Spain

© 2026 Copyright held by the owner/author(s).
ACM ISBN 979-8-4007-2278-3/2026/04
<https://doi.org/10.1145/3772318.3791197>

achieves a balanced accuracy of 0.86, and the ocular-only model shows comparable predictive power. High performers exhibited targeted gaze and adjusted visual sampling, and sustained more stable cardiac activation as demands intensified, with a more positive affective experience. These findings demonstrate the feasibility of cross-session prediction from early physiology, providing interpretable insights into performance variation and facilitating future proactive intervention.

CCS Concepts

• **Human-centered computing** → **User models**; *Empirical studies in HCI*; • **Computing methodologies** → **Machine learning approaches**.

Keywords

Eye tracking; Multimodal physiological signals; Heart rate variability; Performance prediction; Video games

ACM Reference Format:

Yufei Cao, Penny Sweetser, Ziyu Chen, and Xuanying Zhu. 2026. Signals of Success and Struggle: Early Prediction and Physiological Signatures of Human Performance across Task Complexity. In *Proceedings of the 2026 CHI Conference on Human Factors in Computing Systems (CHI '26), April 13–17, 2026, Barcelona, Spain*. ACM, New York, NY, USA, 23 pages. <https://doi.org/10.1145/3772318.3791197>

1 Introduction

User performance is a key indicator of interaction effectiveness, capturing how successfully and efficiently users achieve task goals [26, 47, 104, 108]. This metric is critical across interactive contexts, ranging from high-risk operations such as aviation and driving, where reliable performance is paramount for operational safety [10, 70, 100, 126], to engagement-driven environments including educational platforms and digital games, where sustained achievement supports user motivation and ongoing participation [77, 78, 81]. Beyond functioning as terminal outcomes, performance measures reflect the quality of coupling between user and system during task execution, signalling users' effective coping or emerging struggle in response to task complexity. Anticipating performance outcomes enables interactive systems to provide prospective assessment and support intervention before performance breakdown occurs. This capability is essential for maintaining task continuity as task complexity escalates. Consequently, there is a growing need for interactive technologies to move beyond reacting to manifest errors towards predicting future performance trajectories [1, 35, 120].

Prospective performance forecasting has proven feasible in real-world systems, primarily relying on behavioural metrics (e.g., data logs, user motion, task completion time) [1, 5, 35, 107]. For instance, early predictive models in education can identify students at risk of failing based on their first weeks' learning activities [1], and game telemetry in esports has been used to predict the onset of acute performance decline during competitive play [120]. However, while demonstrating the feasibility of early forecasting of performance trajectories, these behavioural indicators primarily capture what actions are taken but remain opaque with regard to the continuous cognitive processes and hidden physiological costs deployed to sustain performance, such as the mental effort or stress reactivity

occurring between observable actions [23, 62, 106, 106, 121]. This explanatory limitation motivates the use of measures that reflect the covert cognitive and physiological processes supporting task performance.

Ocular and cardiac signals fulfil these requirements by capturing the dynamics of visual behaviour and autonomic activity. Specifically, ocular measures map the spatiotemporal features that reveal how users explore, prioritise, and adapt to task-relevant elements, thereby offering a window into the internal cognitive processes guiding these ongoing actions [56]. Prior work has successfully leveraged eye-movement behaviour to study efficient visual search strategies and attentional guidance in complex interfaces [2, 46, 113], identify visual scanning patterns characteristic of experts versus novices [22, 33, 83], and quantify the mental effort required to maintain performance via pupil dynamics [34, 88, 118, 124]. Complementarily, cardiac measures (e.g., heart rate variability) index autonomic regulation, reflecting how users mobilise physiological resources to manage arousal and stress reactivity under fluctuating task demands [48, 69, 76, 127]. Ocular and cardiac signals jointly capture the continuous interplay between visual information sampling and autonomic regulation that is relevant for task performance, establishing them as promising candidates for early prediction of subsequent performance outcomes. However, it remains unclear whether they are capable of prospective prediction under escalating task complexity in real interaction settings.

Despite the widespread use of ocular and cardiac measures to characterise expertise, workload, and self-regulatory capacity across a range of tasks [33, 37, 58, 69, 83], these applications have primarily focused on identifying users' momentary physiological states to interpret performance variations within the current task conditions. However, such momentary states are highly sensitive to local events and do not reliably indicate the user's overall level of task performance [30, 42], particularly in real-world interactive systems where task demands naturally intensify and interaction proceeds continuously rather than in brief, isolated intervals. To address the gap in research where the early prediction of performance outcomes using physiological signals under evolving task complexity remains underexplored, we propose to prospectively predict performance outcomes using early ocular and cardiac signals under increasing task complexity. We situate our investigation in a digital game environment, which offers an ecologically valid yet controlled setting where performance outcomes (win/loss) arise naturally. These outcomes emerge as complexity progressively escalates, allowing performance to be examined across different levels of task demand. The engaging nature of games sustains participant involvement across continuous sessions and yields authentic data. Game performance outcomes also entail core processes of planning, problem solving, and strategy adaptation that generalise beyond entertainment, making games a powerful testbed for predicting performance outcomes. In this context, we operationalised escalating demands as two complexity stages: a low-complexity stage followed by a high-complexity stage, providing a structured basis for examining how early signals relate to later outcomes.

To complement these physiological indices, subjective affective ratings of valence, arousal, and dominance provide additional context on participants' affective experience and sense of control during gameplay. These measures help situate the observed physiological

patterns within the self-reported affective states across the temporal progression of gameplay. By integrating these measures, our study asks:

- **RQ1.** To what extent can early ocular and cardiac signals predict later performance outcomes as task complexity escalates?
- **RQ2.** How do ocular and cardiac features differ between high- and low-performing groups under increasing task complexity?
- **RQ3.** How do subjective affective experiences and sense of control differ between high- and low-performing groups?

To address these research questions, we conducted a within-subject experiment with 35 participants, recording ocular and cardiac signals while they played a deck-building game consisting of two sessions of increasing complexity. After each session, participants completed affective self-report scales. From the ocular data, we extracted saccade, pupil, and gaze-distribution features, and from the cardiac data, we derived blood volume pulse and heart rate indicators, following established links between these measures and task performance [38, 44, 65, 66, 127]. To assess the predictive performance of ocular and cardiac signals from the low-complexity session in classifying performance outcomes in the subsequent high-complexity session (win/loss), we evaluated ocular-only, cardiac-only, and decision-level fused features under a leave-one-subject-out (LOSO) cross-validation scheme.

Our results show that the fusion model achieved a balanced accuracy of 0.86, demonstrating reliable early prediction of later performance. The ocular-only model performed comparably, whereas the cardiac-only model showed weaker predictive power (balanced accuracy = 0.70). Among the extracted features, gaze distribution, saccade dynamics, and heart rate were the most informative predictors distinguishing high- and low-performing participants. These measures exhibited different temporal trajectories across complexity sessions, providing interpretable context for performance-related differences in visual behaviour and autonomic activity. Self-reports further revealed significant differences in perceived emotion and sense of dominance, which supplemented the physiological evidence.

This study provides the first empirical evidence that physiological signals from the low-complexity session can forecast performance outcomes in the subsequent high-complexity session within a single game context, forming the basis for our contributions to multimodal psychophysiology computing, performance prediction, and applied machine learning in HCI by:

- Demonstrating that early-session ocular and cardiac signals exhibit predictive value for later performance under escalating complexity within the examined game setting, extending prior physiological performance prediction research beyond concurrent state estimation.
- Identifying systematic differences between high- and low-performing groups in ocular indices of attentional control and cardiac indices of autonomic regulation across complexity sessions, characterising task-specific physiological patterns associated with performance regulation.
- Revealing subjective differences in affective experience and sense of control between high- and low-performing groups,

enriching the interpretation of the physiological patterns across the progression of game complexity.

2 Related Work

We investigated the existing body of research on performance prediction in various interactive domains, on the use of multimodal physiological signals to capture performance-related user states, and on modelling approaches for physiological data. Prior studies show that behavioural data and physiological signals can forecast outcomes, but these approaches often rely on short temporal windows and give limited insight into the causes of performance differences. Psychophysiological work demonstrates that cardiac measures index internal regulation, pupil size reflects cognitive and affective states, and eye movements reveal attentional control, yet these signals are rarely combined. Modelling approaches for physiology-based prediction tasks benefit from tree-based ensembles and recurrent sequence models. This body of work shows how early physiological signals can be leveraged to anticipate performance outcomes in interactive tasks.

2.1 Performance Prediction in Interactive Contexts

Performance has been described through measurable outcomes of task execution, encompassing indicators of effectiveness, efficiency, and success under given conditions [16, 28, 47]. As these outcomes reflect the quality of user–system interaction under task demands, recent research across interaction domains has increasingly investigated how predictive models can anticipate performance outcomes.

An increasing body of research in human–computer interaction has leveraged physiological sensing to predict task performance. Heard et al. [41] mapped multimodal physiological signals to workload estimates, which in turn forecasted accuracy and efficiency in supervisory control tasks up to several minutes ahead. Similarly, Guo et al. [35] combined ECG, GSR, EMG, and behavioural indicators (e.g., response timing) to anticipate trust levels in human–robot collaboration before task completion. In competitive eSports, prediction has been investigated at multiple temporal and physiological scales. Smerdov et al. [107] segmented eSports gameplay into temporal windows, using the combination of game logs, physiological signals, and chair-sensor signals to forecast player performance in subsequent segments, within 240 seconds ahead. Minami et al. [79] instead focused on pre-match EEG activity, showing that gamma and alpha oscillations could forecast match outcomes, though interpretability remained constrained to neural correlates of preparation. Beyond predicting outcomes, Wei et al. [120] operationalised the construct of “tilt” by detecting imminent breakdowns in eSports performance, demonstrating that sudden declines could be predicted seconds to minutes in advance from telemetry and physiological markers.

Across these domains, emerging evidence points to the value of early-task windows of physiological data for prospective prediction of performance outcomes. However, existing work has focused on state monitoring or short-term predictions (e.g., seconds ahead) within the same task conditions. While cardiac and neural signals are widely used, ocular measures, closely aligned with information processing and interface interaction, have been comparatively

underexplored as predictors. This creates a need for approaches that (1) assess whether physiological predictors remain informative across phases where task complexity escalates, and (2) integrate ocular and cardiac measures to broaden the predictive scope of physiological sensing.

2.2 Ocular and Cardiac Signals as Predictors of Performance

Psychophysiological research is defined as the use of physiological signals to investigate psychological processes [15]. Among physiological channels, eye movements governed by the central nervous system provide rich indices of visual behaviour during information processing [94]. Heart rate (HR), heart rate variability (HRV), blood volume pulse (BVP), and pupil diameter (PD) are regulated by autonomic nervous system (ANS) activity, indexing physiological arousal within cognitive and emotional contexts.

Eye movements in experimental settings typically comprise fixations and saccades, which represent the core oculomotor mechanisms enabling visual perception through periods of information uptake and rapid gaze shifts across the scene [44, 56]. They have been employed to study the direct reflection of external attention [12, 29, 64, 71, 109], visual search strategies [98], and interface interaction behaviours [2, 31]. The influential “eye–mind assumption” posits that what people fixate on reflects where cognitive processing occurs [50]. Researchers have identified fixation and saccade features as reliable indicators of cognitive performance [6, 44, 91]. Fixation duration and frequency have been identified as reliable indicators of cognitive load [92, 119] and attentional allocation [82, 113]. Saccadic behaviour further indexes visual information processing and processing efficiency [32, 46, 65, 103]. Target selection during saccades is strongly shaped by high-level cognitive factors such as expected rewards and task relevance [83], showing sensitivity to top-down modulation [122]. Under high-load conditions, such as driving [17], video gameplay [73], or online interviews [9], saccades of larger amplitude and higher velocity have been associated with higher stress, increased task complexity, and reduced concentration. As cognitive demands intensify, saccadic efficiency deteriorates, leading to delayed initiation and increased error rates during visual search tasks [65].

At the spatial level, AOI-based gaze distribution analysis has been widely used to examine how visual sampling is allocated across interfaces in interactive environments. Prior studies show that skilled users allocate a greater proportion of gaze to functionally critical regions. For example, in surgical simulation, experts focus more on anatomically important areas [33, 63], and in map-reading tasks, skilled users concentrate fixations on semantically informative regions rather than distributing gaze diffusely across the display [83]. In game-based learning environments, gaze data have been used to track attention to instructional cues and gameplay elements, showing how fixation patterns characterise task-driven allocation of visual resources and support interface design decisions [54].

Cardiac measures provide a complementary index of autonomic activity during task execution. In cognitively demanding tasks, elevated heart rate has been observed alongside higher performance levels, though this benefit diminishes under the highest difficulty

levels [3]. In serial-subtraction tasks, HR rises as participants maintain performance under greater cognitive demands [53]. Similar associations have been reported in interactive contexts such as serious games, where HR increases with cognitive load in parallel with pupil dilation [48]. However, in entertainment gameplay, HR also varies with experiential quality, in which higher HR is linked to greater tension and negatively valenced player experience [24]. HRV, defined as the fluctuation in time between successive heartbeats [112], has long been recognised as a sensitive index of ANS function [45, 57]. Greater resting HRV predicts better cognitive flexibility in older adults [84] and supports working memory performance [37]. Extending these associations to interactive contexts, Lan et al. [60] showed that short-term HRV indices could effectively predict player performance metrics, such as the number of kills, demonstrating the potential of HRV as a predictor of performance in interactive environments. In parallel, BVP, which reflects the volume of blood flowing through peripheral vessels, has been widely employed in studies of stress and cognitive load [40]. Zhou et al. [127] demonstrated that BVP values varied systematically with levels of cognitive load, showing a connection between BVP dynamics and mental demands.

Pupil diameter (PD) refers to the size of the pupil and has been consistently linked to autonomic activity. Classic work by Hess and Polt [43] first showed that pupils dilate in response to interesting relevant stimuli. Libby et al. [64] found that pupil dilation and cardiac deceleration co-occur when a stimulus elicits greater attention and interest, identifying PD as a sensitive indicator of visual orienting during stimulus processing. In addition, a substantial body of work has linked task-evoked PD to mental effort. Studies of cognitive control report that pupil size increases as mental demands rise, such as in adaptive learning [102, 105] and cognitive-load manipulation [34]. These findings describe PD as a reliable marker of the effort involved in inhibiting responses and sustaining working memory [118]. Multimodal studies increasingly incorporate PD with other signals to improve the performance of classification models of user states [68, 125].

Overall, these findings show that ocular measures of saccades, fixations, and gaze allocation capture how users visually access information and distribute attention during ongoing interaction, while cardiac measures provide insight into changes in autonomic activation across different task conditions. These modalities offer complementary perspectives on user state during interaction, supporting their use in models that predict task performance. To characterise participants’ reported experiences.

3 Method

We conducted a within-subject laboratory study in a digital game environment comprising two escalating complexity sessions. During the experiment, we collected ocular and cardiac signals for physiological modelling, as well as a post-session self-report of affective experience for complementary analysis. Using the ocular and cardiac data, we developed a prediction framework encompassing preprocessing, feature extraction, and model development to forecast performance outcomes. In addition, we examined the contribution of individual ocular and cardiac features and visualised

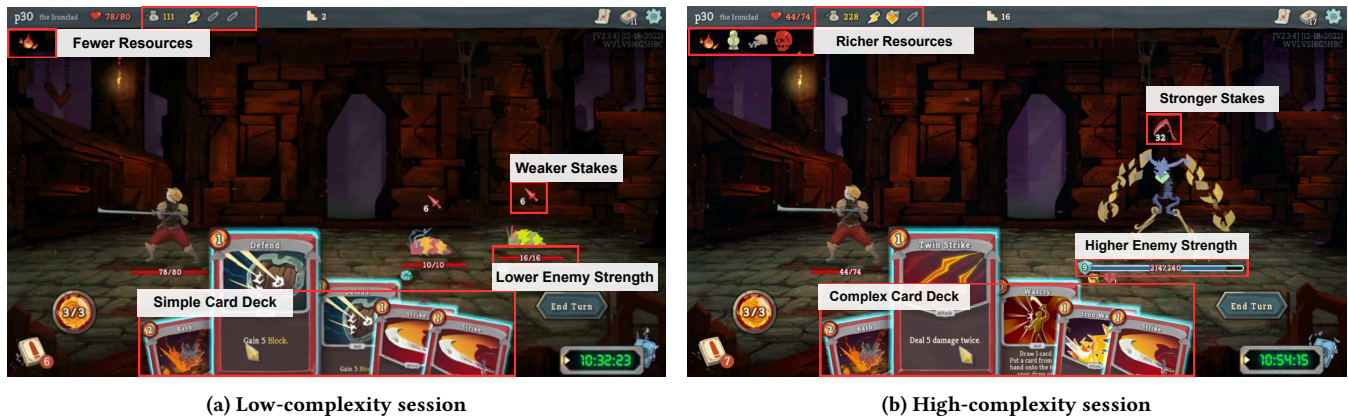


Figure 2: Example game scenes illustrating the two experimental sessions. (a) Low-complexity session, characterised by fewer resources, weaker enemies, and a simple card deck; (b) High-complexity session, featuring more resources available, stronger enemies, and complex cards with intricate effects.

their trends across complexity levels, and the subjective data were analysed separately

3.1 Participants

We recruited 35 participants (16 male, 17 female, 2 non-binary) from the university campus and online platforms. Participants were aged 18–34 years, with 54.3% in the 18–24 range and 45.7% in the 25–34 range. The majority held a bachelor’s degree or higher. To ensure a comparable baseline, only individuals with no prior experience of the game were included. All participants reported normal or corrected-to-normal vision. The study protocol was approved by the university ethics committee, and all participants provided informed consent prior to participation. Participants received either course credit or a voucher as compensation.

3.2 Experiment Design

We conducted a within-subject laboratory experiment using a commercial video game, *Slay the Spire* (Figure 2), dividing the gameplay into two sessions corresponding to lower and higher task complexity. A within-subject design was employed to determine whether early physiological signals could predict later performance under escalating complexity. By keeping the progression fixed for each participant and referencing physiological changes against their own low-demand baseline, the design isolates dynamic adjustments to rising complexity while minimising the influence of stable individual differences.

Slay the Spire [75] is a turn-based deck-building game built around a core loop of strategic card selection, resource management, and adaptive planning. Players act using a customisable deck of cards, where each card represents attacks, defences, or effect actions. During each combat encounter, enemy intent is visible, requiring players to choose cards in response to incoming threats, manage their limited energy and resources, and sequence actions efficiently. Across the run, players progress through successive encounters by building and refining their deck, culminating in a boss fight that concludes the level.

The game offers a progressive task structure in which combat demands escalate from normal battles to a final boss that appears at the end of the first level, creating a natural increase in overall task complexity as players advance (Figure 2, left: normal battle; right: boss battle). Early battles typically feature simpler decision requirements, fewer interacting resources, and enemies with straightforward attack patterns. In contrast, the boss encounter imposes substantially higher demands, featuring enemies with greater durability, more punishing attack cycles, and unique mechanics that disrupt the player’s deck or introduce additional constraints, requiring more elaborate reasoning over a richer set of interdependent cards, resources, and combinational effects. Accordingly, the experiment distinguished between two sessions: a low-complexity session encompassing the pre-boss encounters, and a high-complexity session corresponding to the final boss encounter. This design reflects the game’s inherent progression rather than imposed manipulation of task difficulty, and creates a temporal structure in which early-stage physiological patterns under lower demands can be used to forecast performance outcomes under later, higher task complexity. This escalation aligns with cognitive load theory, in which task difficulty rises with increases in element interactivity [111]. Early encounters involve low interactivity and offer a lower-load segment that precedes the sharp rise in cognitive demands, whereas later encounters require coordinating many interdependent elements, making performance increasingly sensitive to individual differences.

To ensure comparability across participants, we fixed the character selection and level map using the game’s customisation options and applied a constant run seed, producing an identical layout and enemy sequence across all runs. The entire experiment used only the first level with a fixed map layout. Each participant began with a short built-in introductory sequence for familiarisation before entering the main combat stages. The low-complexity session lasted up to 25 minutes, whereas the high-complexity session lasted up to 15 minutes. Each participant completed a single uninterrupted run. If the player’s health points were depleted at any point, the run terminated without restart and was coded as a loss. Reaching the final boss and defeating it was coded as a win. Participants

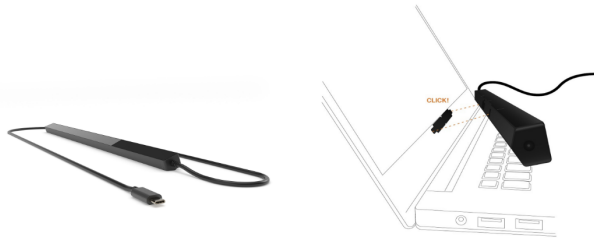


Figure 3: Eye tracking system (Tobii Pro Fusion).



Figure 4: Cardiac recording device (Empatica EmbracePlus Wristband).

were explicitly instructed that their goal was to defeat the boss, ensuring consistent motivation and engagement across the game progression.

3.3 Apparatus and Signals

Ocular data were recorded with the Tobii Pro Fusion, a screen-based binocular eye tracker (see Figure 3) [116]. The device sampled at 250 Hz and offered high spatial precision. It was integrated with a 23.8-inch monitor (1920 × 1080 resolution), and participants were seated approximately 60 cm from the screen without a chin rest, allowing for natural head movement. We used Tobii Pro Lab software for calibration and data collection [117]. We selected a screen-based tracker to support natural interaction, ensuring stable gaze estimation while maintaining ecological validity for seated game play.

Cardiac data were recorded using the EmbracePlus, a wearable multisensor device developed by Empatica Inc (see Figure 4) [27]. The EmbracePlus records BVP via an optical photoplethysmography (PPG) sensor to capture cardiovascular pulse activity. BVP was sampled at 64 Hz, with data acquisition managed via the Empatica mobile app and uploaded to the Empatica Research Portal. We selected a wrist-worn device to ensure comfort and minimise intrusiveness, enabling long-duration recording without distracting participants during gameplay. The wrist-based form factor also aligns with consumer smartwatches, and using cost-effective, readily accessible technology enables investigating whether physiological sensing commonly found in everyday smartwatches is capable of supporting performance prediction in interactive environments.

3.4 Procedure

The overall structure of the experimental sessions is shown in Figure 5. Participants first completed a demographic questionnaire.

At the beginning of the experiment, each participant was fitted with an Empatica wristband on the non-dominant wrist and then completed a 9-point calibration and validation procedure in Tobii Pro Lab. Calibration was repeated if the mean accuracy exceeded 1.0° or if data loss was greater than 10%. All participants met these criteria before proceeding. The first game session began with a built-in tutorial, during which participants could ask questions about the game mechanics. Following this session, they completed a game difficulty scale and an affective experience scale. Before the second session, calibration was repeated to ensure eye-tracking quality. Finally, the second game session concluded with the same self-report questionnaires.

3.5 Subjective Measures

Perceived game task difficulty was assessed using a 5-point Likert scale, where 1 indicated very easy and 5 indicated very hard. Participants rated the overall difficulty of both the low-difficulty and high-difficulty sessions. The questionnaire item was phrased as: "Please rate your overall experience regarding the difficulty level of the first game session."

Affective experience was measured using the Self-Assessment Manikin (SAM) [85], a non-verbal pictorial instrument that assesses three dimensions of emotion. Valence captures the degree of pleasantness, ranging from unpleasant (1) to pleasant (5). Arousal reflects the level of physiological activation, ranging from calm (1) to excited (5). Dominance represents the perceived sense of control, ranging from low control (1) to high control (5). Participants were instructed to select the figure that best represented their emotional state during the session. The item was phrased as: "Please choose from the above figures which best matches your state when you play the game."

4 Signal Processing and Feature Engineering

To enable predictive modelling from physiological input, we transformed raw ocular and cardiac signals into structured features via a multi-stage pipeline comprising denoising, segmentation, and modality-specific windowing, followed by feature extraction, fusion, and selection to prepare the data for classification.

4.1 Feature Categories

To structure the feature space for subsequent modelling, we categorised the features into ocular and cardiac groups, summarised in Table 1 and Table 2. The full set of ocular and cardiac features, along with their statistical definitions, is provided in Appendix B.

The ocular group consists of pupillometry, fixation, and saccadic behaviours, reflecting pupil-linked arousal and visual scanning dynamics [32, 82, 118]. In addition, gaze distribution to predefined areas of interest (AOI) was included to capture attention allocation to task-critical interface regions that are essential for strategic choices [44]. AOIs were defined as several interface elements, including the hand cards (available actions), the top toolbars displaying potions (consumable items) and relics (persistent upgrades). A detailed illustration of these AOIs is provided in Appendix D.

The cardiac group consists of heart-related metrics, reflecting general arousal, autonomic regulation, and peripheral cardiovascular reactivity [49, 112, 127].

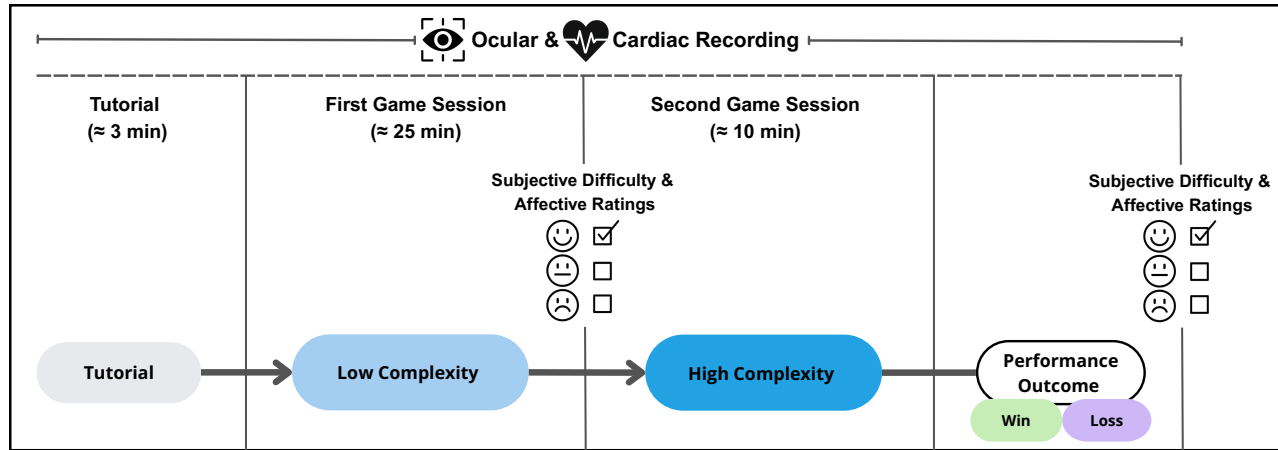


Figure 5: Experimental procedure with annotated session structure and physiological recording.

Table 1: Overview of extracted ocular features and their functional roles.

Category	Feature Names	Functional Role
Fixation	Fixation Duration, Fixation Count	Periods where gaze remains relatively stable, indicating focused attention.
Saccade	Saccade Amplitude, Saccade Duration, Saccade Velocity, Saccade Count, Saccade to fixation ratio	Rapid eye movements between fixations, reflecting visual scanning and search behaviour.
Pupillometry	Pupil Diameter	Pupil size changes, associated with cognitive effort and emotional arousal.
AOI Features	AOI Hit Rate, AOI Proportion	Distribution and allocation of visual attention across predefined regions of interest on the game interface.

Table 2: Overview of extracted cardiac features and their functional roles.

Category	Feature Names	Functional Role
Heart Rate Metrics	Heart Rate, Heart Rate Range	Reflect overall cardiovascular activation.
Heart Rate Variability Metrics	Root Mean Square of Successive Differences (RMSSD), Mean NN Interval	Reflect autonomic nervous system regulation.

4.2 Data Preprocessing

Raw ocular and cardiac signals were preprocessed through a series of steps. First, all physiological time series were offline-aligned to the game timeline by synchronising the signal timestamps with a millisecond-precision on-screen clock plugin. Based on this alignment, each participant’s data were segmented into the tutorial, low-complexity, and high-complexity sessions.

Raw pupil diameter data were cleaned to remove artifacts and sensor noise. Periods of signal loss (e.g., blinks), which accounted for less than 5% of the dataset, were corrected using linear interpolation to maintain temporal continuity. A fourth-order Butterworth low-pass filter (cutoff = 4 Hz) was then applied to suppress high-frequency noise. For gaze metrics, raw screen-coordinate data (X, Y) were used to compute saccade kinematics. Velocity profiles were smoothed using a Savitzky–Golay filter [101] with a 13-sample window and a third-order polynomial, reducing jitter and improving the robustness of velocity estimation. Data points located outside the display boundaries were removed to ensure that only valid on-screen gaze behaviour was analysed.

Raw BVP signals were filtered using a sixth-order Butterworth low-pass filter. A 3 Hz cutoff to remove high-frequency noise and motion-induced artifacts. Zero-phase forward–backward filtering (filtfilt) was applied to eliminate phase distortion, preserving the temporal alignment of systolic peaks with the original physiological events.

4.3 Feature Extraction

To transform the cleaned ocular and cardiac time series into interpretable measures, feature extraction was carried out separately for each modality.

Ocular features encompassed pupillometry measures, saccade, fixation metrics, and AOI-based gaze distribution. Pupil diameters were obtained directly in millimetres for both eyes. Saccade amplitude and velocity were calculated from the Euclidean distance between successive gaze points in the x–y plane relative to movement duration. Saccade and fixation counts were determined by

marking the onset of each event, while fixation durations were derived from gaze duration values. AOIs were defined from in-game screenshots using automated image processing (OpenCV-based template matching and contour extraction) [13], yielding pixel and normalised coordinates for two fixed toolbar elements. Gaze samples were compared against these AOI boundaries to produce two indices: the proportion of gaze samples within each AOI and the frequency of AOI hits. Based on preliminary testing of window lengths, we used a 500 ms sliding window with a 250 ms step for ocular feature calculations. This configuration yielded stronger predictive performance and provides a practical trade-off between measurement stability and the temporal resolution required to capture task-evoked changes [87], while remaining sufficient for tracking rapid fluctuations in pupil size and eye-movement dynamics in our experimental settings [44].

Cardiac features were derived from the BVP signals using the NeuroKit2 package [72, 114]. The package detects individual heartbeats and computes inter-beat intervals (IBIs), defined as the time between successive cardiac cycles [89]. From the IBIs, we calculated HR and two time-domain HRV indices: RMSSD and MeanNN. All cardiac features were computed in non-overlapping 15-second windows to ensure the inclusion of a sufficient number of cardiac cycles for estimating heart rate and time-domain variability metrics. Previous work has shown that 10-second ultra-short recordings provide acceptable accuracy for estimating these measures [7, 80].

From these measurements, we extracted 35 features in total, comprising 29 ocular features and 6 cardiac features. Detailed computation procedures and statistical definitions for these ocular and cardiac features are provided in Appendix B.

Following the computation of ocular and cardiac features, a within-subject z-score normalisation was applied to standardise feature distributions, defined as subtracting each participant's mean and dividing by their standard deviation across all windows. This per-participant normalisation centred each feature distribution around zero and scaled it by its own variability, thereby removing baseline differences across individuals while preserving the relative fluctuations that reflect within-subject dynamics.

4.4 Feature Selection and Dataset Construction

Feature selection was conducted iteratively using statistical filtering, model-based ranking, and ablation assessment. We initiated with statistical filtering, where descriptive statistics and the Mann–Whitney U (MWU) test [20] were applied to the unimodal feature sets. Shapiro–Wilk tests [86] and Quantile–Quantile (Q–Q) plots [86] were used to assess normality prior to the MWU test, followed by tests for equal variance. In addition, we incorporated model-based feature importance scores from tree-based learners to prioritise informative predictors and remove redundant features. Candidate subsets were then evaluated in ablation experiments to assess how the removal of specific feature categories affected generalisation performance. This iterative procedure guided the final retained features. The resulting multimodal feature set comprised 10 ocular features and 2 cardiac features. A complete summary of all extracted features and the final subset is provided in Appendix C. The final dataset contained 35 participant-level instances, with the performance classes nearly balanced (win: 19, loss: 16).

5 Predictive Modelling

To evaluate whether early physiological responses forecast subsequent performance, we built independent predictive models from ocular and cardiac features and then combined their outputs through a decision-level fusion framework. Generalisability was assessed using a LOSO protocol. Figure 6 shows the processing pipeline for ocular, cardiac and fusion modalities. Both data streams undergo preprocessing, feature engineering, and model training independently. The ocular stream extracts pupil diameter, saccade, fixation, and gaze features, whereas the cardiac stream extracts features derived from BVP, HR, and HRV. Each modality produces a probability estimate (P_{ocular} , P_{cardiac}). The two probability outputs are then combined using a decision-level fusion strategy for final performance prediction (win or loss).

5.1 Classification Models

We trained three supervised classifiers: XGBoost [18], CatBoost [93], and Linear SVM [21]. Tree-based ensembles (XGBoost, CatBoost) were selected for their ability to model non-linear interactions in physiological data. Additionally, a Linear SVM was trained as a baseline to assess whether the decision boundary could be linearly separated. Hyperparameters for each model (e.g., tree depth, learning rate, regularization strength) were optimised using grid search within each training fold. The detailed tuning ranges and final configurations are provided in Appendix A.

5.2 Decision-Level Late Fusion

To combine the predictions from ocular and cardiac models, we adopted a decision-level late fusion. This approach is appropriate for multimodal signals that differ in temporal resolution, statistical properties, and windowing structures. Decision fusion aggregates independently trained model outputs and therefore accommodates heterogeneous physiological modalities without requiring shared representations [55, 59].

Our fusion approach follows a consensus-first strategy [4, 25, 128]. A *consensus* is identified when the two modalities independently produce the same subject-level label ($\hat{y}_{\text{ocular}} = \hat{y}_{\text{cardiac}}$); this prediction is retained as a high-confidence agreement. These consensus subjects retain their agreed-upon labels without further fusion. Only disagreement cases are passed to downstream fusion operators. This strategy concentrates fusion capacity on conflicts between modalities and reduces unnecessary decision noise, consistent with the broader ensemble-learning principle that classifier agreement implies reliability [128].

For each subject, both modalities output a probability p and a subject-specific decision threshold τ chosen on the training folds to maximise balanced accuracy. A hard decision was obtained by thresholding τ , i.e., $\hat{y} = 1$ if $p \geq \tau$ and 0 otherwise. The use of personalised thresholds τ ensures that each individual's decision boundary reflects their own score distribution.

Conflict subjects ($\hat{y}_{\text{ocular}} \neq \hat{y}_{\text{cardiac}}$) undergo fusion. For these cases, we employ a stacking-based late fusion approach. A meta-classifier (XGBoost) learns a non-linear mapping from the two modality-specific confidence scores [p_{ocular} , p_{cardiac}] to a fused score estimate, following established methods of stacked generalisation [123, 128]. A fusion-specific threshold τ_{fusion}^* is then re-estimated

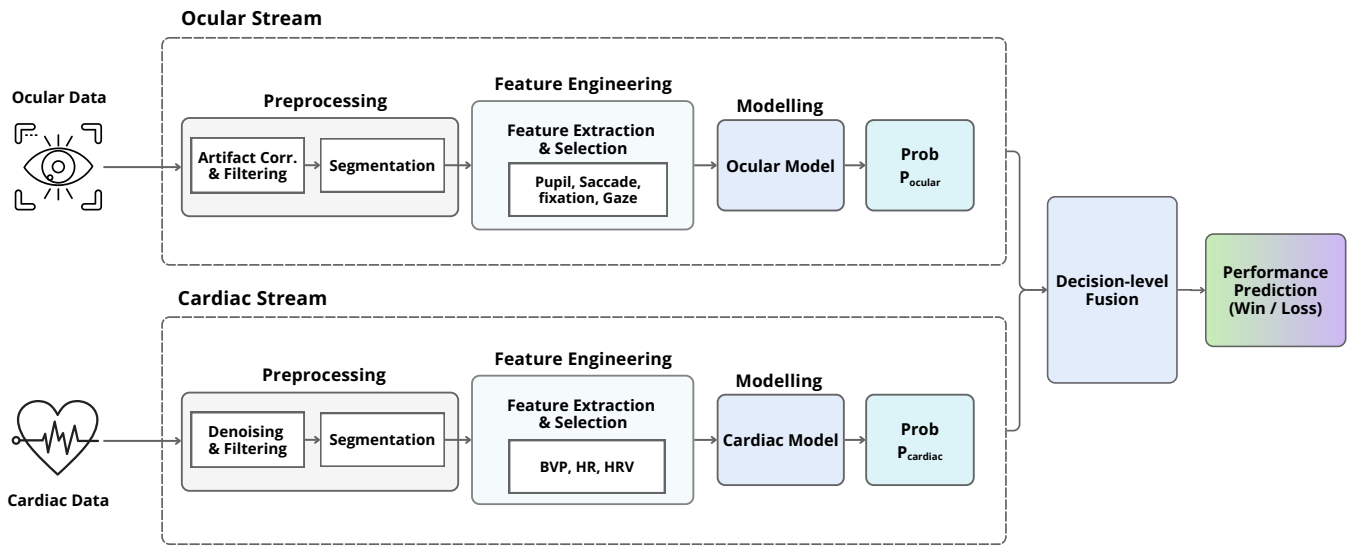


Figure 6: Processing framework integrating ocular, cardiac, and fused modalities.

on the training folds to maximise balanced accuracy, calibrating the fused decision boundary to the score distributions of conflict cases.

5.3 Cross-Participant Evaluation (LOSO)

We adopted a LOSO across-subject evaluation protocol to assess model generalisability. In each fold, one participant was held out for testing, and the model was trained on data from all remaining participants. Inference was performed using only the held-out participant’s low-complexity session signals to predict their performance outcome in the subsequent high-complexity session, providing a strict test of prospective prediction under escalating task demands. Within each training fold, hyperparameter tuning and decision-threshold optimisation were performed through an inner participant-wise cross-validation loop on the training set, selecting the threshold that maximised balanced accuracy. After tuning, the model was retrained on the full training fold and evaluated on the held-out participant. Class imbalance between win and loss outcomes was addressed by applying class weighting within the tree-based models. Finally, window-level probabilities were aggregated via logit-mean pooling to produce a single participant-level prediction. Performance was reported using Balanced Accuracy (BAcc), Macro-F1, Macro-Precision (Macro-Pr), Macro-Recall (Macro-Re), and Matthews Correlation Coefficient (MCC).

6 Results

We first present the self-reported task complexity and affective experience measures. We then evaluate the predictive performance of ocular, cardiac, and fused models. Finally, we analyse the key ocular and cardiac predictors across performance groups, illustrating both overall differences and their temporal trajectories across task stages.

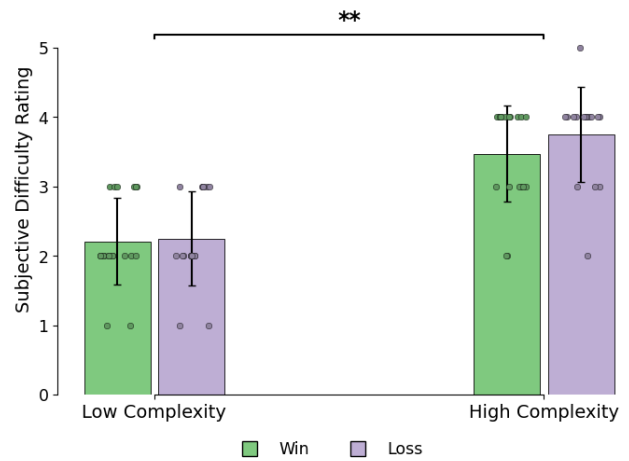


Figure 7: Subjective difficulty ratings across game sessions. Bars represent mean ratings (\pm SD), separated by Low Complexity and High Complexity sessions, with performance groups shown as grouped bars (Win = high-performing; Loss = low-performing). Dots indicate individual participants’ ratings. Asterisks indicate significant difference between sessions (** $p < .01$).

6.1 Self-reported Task Difficulty and Affective Experience across Complexity Levels

To examine perceived task demands across two sessions, subjective difficulty ratings were analysed across game complexity sessions using independent-samples t -tests (Figure 7). On average, difficulty ratings were 2.23 ± 0.65 in the Low Complexity session and 3.60 ± 0.69 in the High Complexity session across all participants. Ratings were significantly higher in the High Complexity session than in the

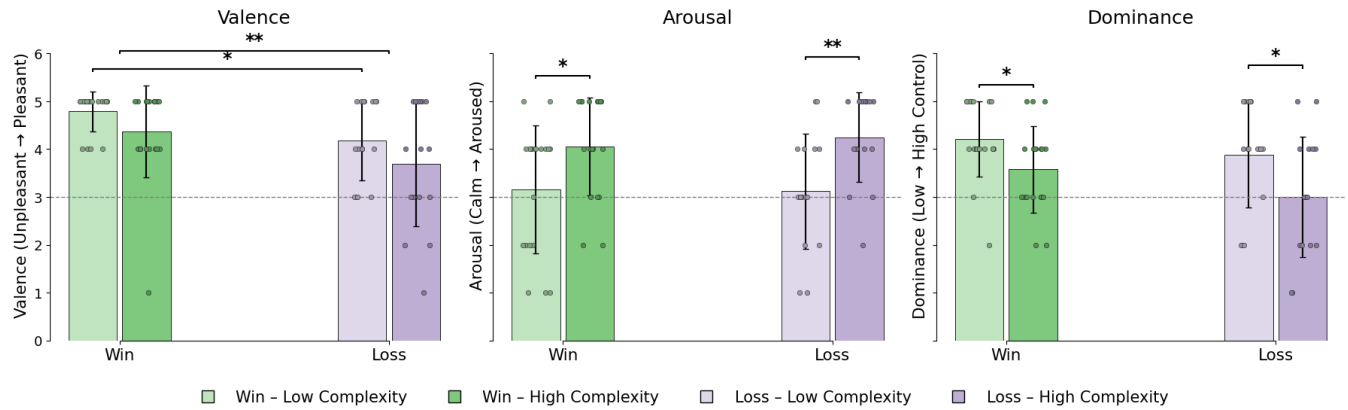


Figure 8: Subjective ratings on the SAM scales grouped by performance (Win = high-performing; Loss = low-performing). Bars show mean (\pm SD), with dots indicating individual participants. Left: Valence (0 = unpleasant, 5 = pleasant). Middle: Arousal (0 = calm, 5 = aroused). Right: Dominance (0 = low control, 5 = high control). Asterisks indicate significant differences ($p < .01$, * $p < .05$).**

Low Complexity session ($p < .01$). In addition, visual inspection showed that participants in the low-performing group reported more ratings at the upper end of the difficulty scale compared to the high-performing group. Within each complexity level, no significant differences were observed between performance groups (Low Complexity: high = 2.21 ± 0.63 vs. low = 2.25 ± 0.68 ; High Complexity: high = 3.47 ± 0.70 vs. low = 3.75 ± 0.68).

Subjective ratings on the SAM scales were analysed using independent samples t -tests. Tests examined (1) between-group differences (high- vs. low-performing participants) within each complexity condition; (2) within-group differences between complexity conditions for each performance group; and (3) overall between-group differences across complexity conditions. Results are summarised in Figure 8.

Valence, ranging from unpleasant/negative to pleasant/positive, showed a significant performance effect across complexity levels, with the high-performing participants reporting higher valence (4.58 ± 0.76) than the loss group (3.94 ± 1.11), $p < .01$. In the Low Complexity condition, the high-performing group reported more positive valence (4.79 ± 0.42) than the low-performing group (4.19 ± 0.83), $p < .05$.

Arousal, ranging from calm and relaxed to highly aroused, showed a significant effect of task complexity. In the high-performing group, arousal was significantly higher in the High Complexity condition (4.05 ± 1.03) than in the Low Complexity condition (3.16 ± 1.34), $p < .05$. A similar effect was observed in the low-performing group (High Complexity: 4.25 ± 0.93 ; Low Complexity: 3.12 ± 1.20), $p < .01$.

Dominance, reflecting the degree of control (submissive to dominant), was consistently higher in the Low Complexity condition compared to the High Complexity condition across both performance groups. The high-performing group reported higher dominance in Low Complexity (4.21 ± 0.79) than in High Complexity (3.58 ± 0.90), $p < .05$, and the low-performing group showed the same pattern (Low Complexity: 3.88 ± 1.09 ; High Complexity: 3.00 ± 1.26), $p < .05$. Although dominance ratings were consistently higher for

the high-performing group, no overall performance-group effect was observed (win: 3.89 ± 0.89 ; loss: 3.44 ± 1.24 ; $p = .088$).

6.2 Predictive Performance Analysis

Predictive performance was assessed across ocular, cardiac, and fused modalities under a cross-subject evaluation. Classification outputs were obtained at the participant level. Class-wise outcomes and component contributions were then examined to characterise model errors and the role of key features.

6.2.1 Cross-Subject Classification Performance. We evaluated three classifiers (CatBoost, XGBoost, Linear SVM) using a cross-subject LOSO protocol across the ocular, cardiac, and fused models. All results are based on the final selected configurations after model tuning and feature selection. Table 3 reports balanced accuracy, precision, recall, macro-F1, and MCC, while Figure 9 visually summarises the performance comparison of the tree-based models across modalities.

Across all models, the ocular feature set yielded the strongest unimodal performance. CatBoost achieved a balanced accuracy of 0.83 (SE = 0.06) and an MCC of 0.66, and XGBoost performed similarly (BAcc = 0.80, MCC = 0.54). Cardiac features provided weaker predictive value. The best-performing cardiac model, XGBoost, achieved a balanced accuracy of 0.70 (SE = 0.07) with an MCC of 0.42. The fused model produced the best overall cross-subject generalisation: CatBoost reached a balanced accuracy of 0.86 (SE = 0.05) and an MCC of 0.72, while XGBoost showed comparable improvements (BAcc = 0.83, MCC = 0.66). Across all three modalities, the Linear SVM consistently performed near chance level (BAcc \approx 0.50–0.57, MCC \approx 0–0.27), showing limited capacity to model the non-linear structure present in the physiological features.

Figure 10 presents the confusion matrices for the ocular-only and fused models to detail classification accuracy across groups. The ocular model correctly identified 12 of the 16 actual 'Loss' cases, misclassifying 4 cases as 'Win' (false positives). In comparison, the fused model correctly identified 14 'Loss' cases, reducing the

Table 3: Cross-subject LOSO performance across the ocular, cardiac, and fused feature sets for all models. The table reports the best subject-level results obtained under LOSO, including balanced accuracy, macro-precision, macro-recall, macro-F1, and MCC.

Modality	Model	BAcc	Macro-Pr	Macro-Re	Macro-F1	MCC
Ocular	CatBoost	0.83	0.83	0.82	0.83	0.66
	XGBoost	0.80	0.77	0.76	0.79	0.54
	Linear SVM	0.57	0.79	0.56	0.48	0.27
Cardiac	CatBoost	0.66	0.67	0.66	0.66	0.33
	XGBoost	0.70	0.72	0.70	0.70	0.42
	Linear SVM	0.50	0.27	0.50	0.35	0.00
Fused	CatBoost	0.86	0.89	0.84	0.87	0.72
	XGBoost	0.83	0.88	0.79	0.83	0.66
	Linear SVM	0.50	0.27	0.50	0.35	0.00

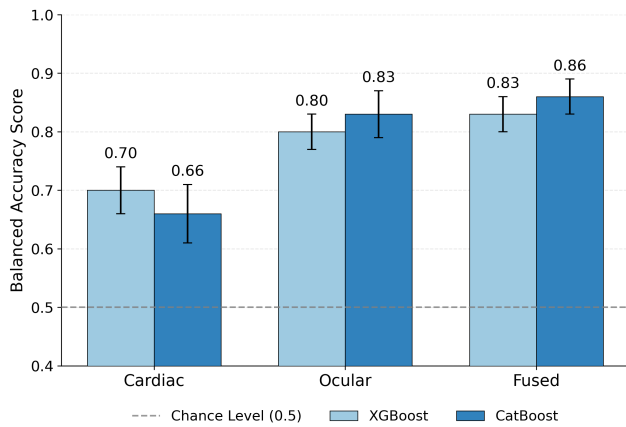


Figure 9: Cross-subject classification performance (balanced accuracy) comparison across modalities. The grouped bars illustrate the incremental predictive power from unimodal (cardiac, ocular) to multimodal (fused) approaches. CatBoost and XGBoost are shown as the top-performing classifiers

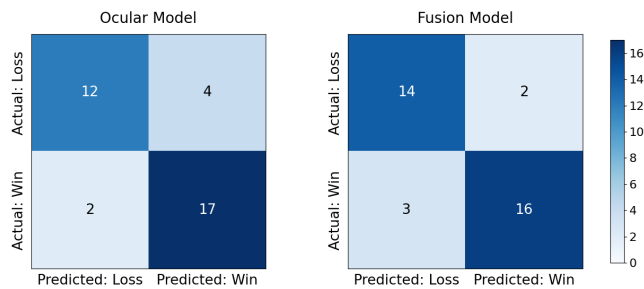


Figure 10: Confusion matrices for the ocular (left) and fused (right) models, selected as the top-performing classifiers from the cross-subject evaluation.

Table 4: Ablation of ocular feature modules, where one component is removed at a time. Δ BAcc denotes the change in balanced accuracy relative to the full ocular model. The row \ corresponds to the full ocular model ($N = 35$, LOSO).

Component Removed	BAcc	Macro F1	MCC	Δ BAcc
\	0.83	0.83	0.66	0.00
Pupil	0.83	0.83	0.66	0.00
Fixation	0.83	0.83	0.66	0.00
Saccade	0.69	0.68	0.37	0.14
AOI Gaze	0.40	0.39	-0.22	0.43

number of false positives to 2. Although the correct identification of 'Win' cases decreased slightly from 17 to 16, the integration of cardiac data produced a net increase in the accurate classification of the low-performing group.

6.2.2 Ablation Study. To evaluate the contribution of specific model components, we conducted ablation studies at two levels: (1) a module level analysis within the ocular modality to determine the predictive power of distinct feature groups, and (2) an architecture level analysis to assess the necessity of the consensus mechanism in the fusion model.

For the ocular model, we defined four key functional components: (1) pupil-based measures, (2) fixation statistics, (3) saccade dynamics, and (4) gaze allocation across AOIs. We performed ablation tests by iteratively removing one component (including all associated features) and evaluating the resulting model. In each variant, only the targeted component was excluded while all remaining components were kept intact. All experiments followed the same cross-subject LOSO protocol, where each fold withheld one participant for testing. To ensure fair comparison, all model configurations, hyperparameters, and threshold-selection procedures were kept consistent with the full ocular model. As shown in Table 4, the ocular modality exhibited a clear internal structure. Some components provided redundant support, whereas others were essential for maintaining predictive reliability. Removing either the pupil features or fixation metrics produced no measurable

Table 5: Ablation of the consensus check in the stacking architecture, where one component is removed at a time. Δ BAcc denotes the change in balanced accuracy relative to the full fusion architecture. The row \ corresponds to the full fusion architecture ($N = 35$, LOSO).

Component Removed	BAcc	Macro F1	MCC	Δ BAcc
\	0.86	0.86	0.72	0.00
Consensus Check	0.77	0.77	0.54	0.09

degradation, with accuracy remaining at 0.83. In contrast, excluding saccade dynamics resulted in a substantial drop to 0.69. The largest degradation occurred when removing AOI-based gaze allocation, where accuracy fell to 40 percent. These results show that while basic ocular features contribute marginally, performance-critical information is carried primarily by saccadic behaviour and gaze allocation across task-relevant regions.

We also evaluated the contribution of the consensus mechanism within the full fusion architecture. We compared the full model with a variant that omitted the consensus check, where the meta-classifier was applied to all samples regardless of unimodal agreement. As presented in Table 5, removing the consensus step led to a drop in performance: balanced accuracy decreased from 0.86 to 0.77 (Δ Bacc = 0.09), with macro-F1 and MCC dropping from 0.86 to 0.77 and from 0.72 to 0.54, respectively. These results indicate that applying the meta-classifier only to disagreement cases yields higher performance than applying it to all samples.

6.3 Dynamics of Ocular and Cardiac Features across Performance Groups

To interpret the predictive model, we examined the contribution of ocular and cardiac features using the feature-importance profiles of the best-performing model for each modality. Specifically, CatBoost was used to extract the importance of ocular features, and XGBoost was used for cardiac features. From these importance profiles, we identified the top-ranked features and selected a subset that aligned with established physiological and task-related interpretability. In total, five ocular features and two cardiac features were identified as the most relevant predictors in the unimodal models. Group differences in these features were analysed using independent-samples t -tests or Mann–Whitney U -tests, with the test choice determined by Shapiro–Wilk normality assessment. The full importance scores for all features are provided in Appendix E (Table 11). Figure 11 illustrates cardiac indices. Mean heart rate (panel A) demonstrated a relatively compact interquartile range but a pronounced upper tail in the high-performing group compared with the low-performing group, although the difference did not reach statistical significance. Heart rate range (panel B) exhibited greater dispersion, with the low-performing group showed an upward shift with a higher median, however, this difference was not statistically significant.

Figure 12 presents the temporal trajectories of cardiac features across tutorial, low-complexity, and high-complexity sessions, separated by performance groups. For mean heart rate (panel A), the

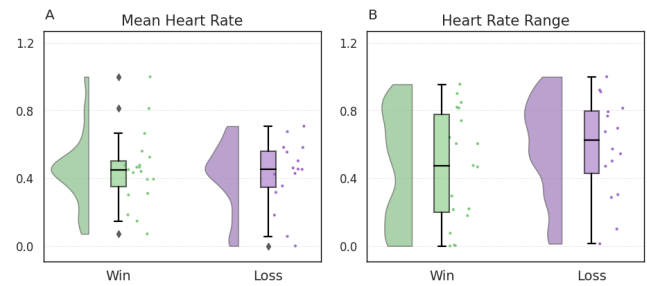


Figure 11: Raincloud plots of cardiovascular features comparing performance groups (Win = high-performing; Loss = low-performing). (A) Mean heart rate. (B) Heart rate range. For all panels, raincloud plots depict individual datapoints (dots), probability density (violin), and boxplots summarising the median and interquartile range.

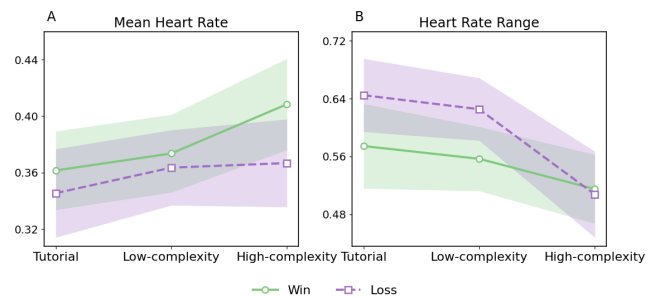


Figure 12: Dynamic trends of cardiac features across three phases (tutorial, low-complexity, high-complexity), comparing performance groups (Win = high-performing; Loss = low-performing). Lines show group means with shaded bands indicating ± 1 SEM.

high-performing group showed a steady increase from the tutorial to the high-complexity session. The low-performing group displayed a similar upward trajectory but remained lower at every stage. The separation between groups widened at higher complexity. For heart rate range (panel B), both groups demonstrated a monotonic reduction across sessions. The low-performing group maintained larger heart rate ranges than the high-performing group at all stages, with the largest numerical separation in the tutorial phase. However, no session showed statistically reliable differences.

Figure 13 illustrates ocular indices. (A) For AOI gaze proportion (potions), a significant between-group difference was observed ($p < .05$). The high-performing group showed a higher median viewing rate with a broader spread towards higher values, while the low-performing group's values were more concentrated at the lower end. (B) For AOI gaze proportion (hand cards), no significant between-group difference was detected. The high-performing group showed a slightly higher median viewing proportion with more dispersed samples across the mid-range, whereas the low-performing group exhibited a narrower distribution centred around

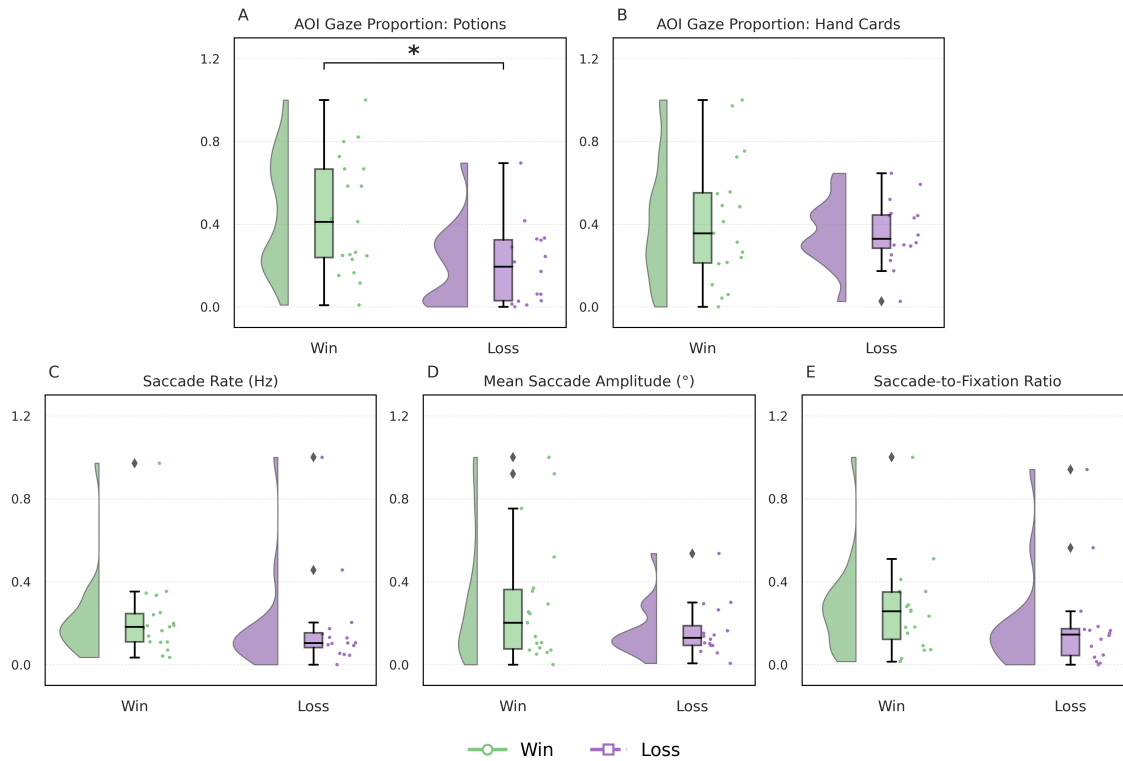


Figure 13: Raincloud plots of ocular features comparing performance groups (Win = high-performing; Loss = low-performing). (A) AOI gaze proportion: Potions. (B) AOI gaze proportion: Hand Cards. (C) Saccade rate (Hz). (D) Mean saccade amplitude (°). (E) Saccade-to-fixation ratio. For all panels, raincloud plots depict individual datapoints (dots), probability density (violin), and boxplots summarising the median and interquartile range. Asterisks indicate significant differences ($*p < .05$).

lower gaze proportions. (C) Mean saccade rate did not differ significantly between groups, but showed a trend towards higher values in the high-performing group ($p = 0.08$). The high-performing group exhibited higher medians and longer upper tails, whereas the low-performing group remained centred at lower values. (D) Mean saccade amplitude did not differ significantly between groups. The high-performing group showed a higher median and a slightly wider interquartile range, whereas the low-performing group had lower central tendencies and reduced spread. (E) The saccade-to-fixation ratio did not reach statistical significance between groups ($p = 0.06$), but showed a clear upward shift in the high-performing group. The high-performing group exhibited a higher median, with the interquartile range centred at higher values than the low-performing group.

Figure 14 presents the temporal trajectories of ocular features. (A) AOI gaze proportion (potions) increased progressively across sessions in both groups. The high-performing group exhibited consistently higher values, with significant between-group differences emerging from the low-complexity session onward ($p < .05$). While both groups showed comparable baselines in the tutorial phase, the high-performing group demonstrated a steeper increase and reached the highest gaze proportion in the high-complexity session. (B) AOI gaze proportion (hand cards) increased progressively across sessions for both groups. The two groups showed

similar levels during the tutorial and low-complexity phases. A divergence emerged in the high-complexity session, where the high-performing group showed a significantly larger increase and achieved a higher proportion than the low-performing group ($p < .05$). (C) Saccade rate showed distinct patterns between groups. Both groups began at comparable levels in the tutorial phase, after which the high-performing group exhibited a steady increase, showing an upward trend relative to the low-performing group in the low-complexity session ($p = 0.06$). The low-performing group remained relatively stable and showed a slight decrease in the high-complexity session, resulting in increasing group divergence. (D) Mean saccade amplitude displayed different trajectories between groups. The high-performing group increased from the tutorial to the low-complexity session, followed by a sharp decline in the high-complexity session. In contrast, the low-performing group exhibited an opposite trajectory, with an initial decrease followed by a subsequent increase. No statistically significant differences were found across sessions. (E) The saccade-to-fixation ratio increased across sessions for the high-performing group, rising most prominently in the high-complexity phase. A trend towards higher values in the high-performing group was observed in the low-complexity session ($p = 0.08$). By contrast, the low-performing group showed minimal change across stages, maintaining a nearly flat trajectory.

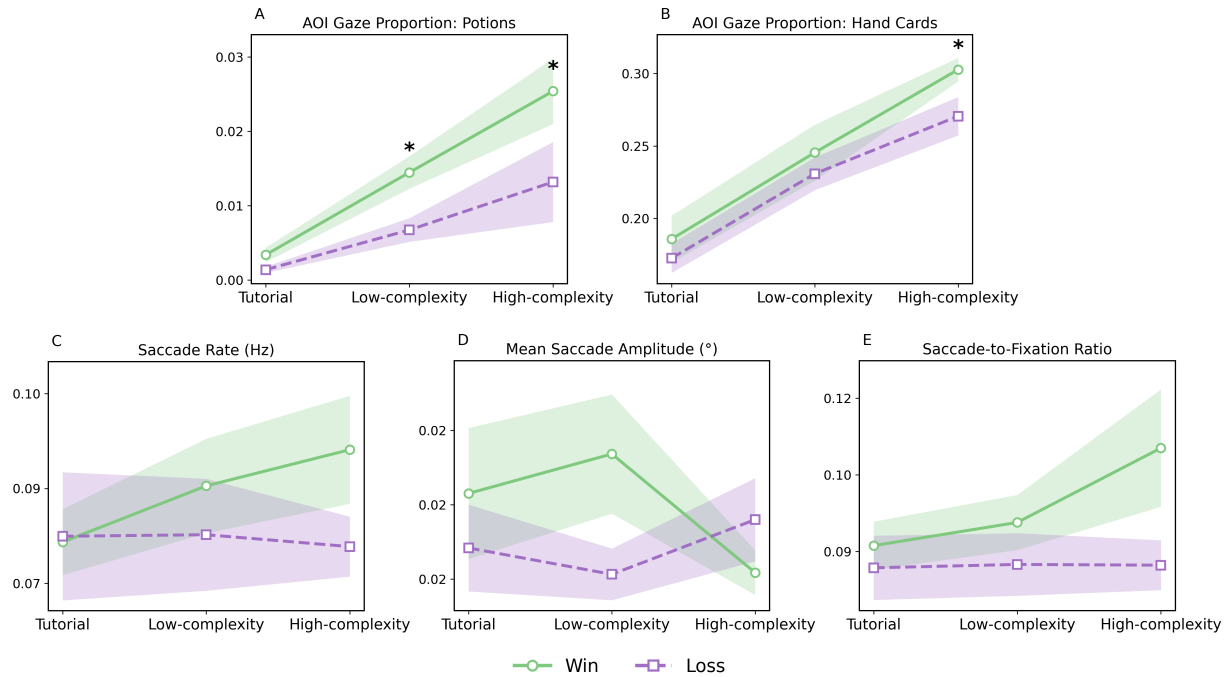


Figure 14: Dynamic trends of ocular features across three phases (tutorial, low-complexity, high-complexity), comparing performance groups (Win = high-performing; Loss = low-performing). Lines show group means with shaded bands indicating ± 1 SEM. Asterisks indicate significant between-group differences at each session ($p < .05$).

7 Discussion

We evaluated the feasibility of using early physiological signals for performance prediction across task phases. In our study, participants completed two consecutive sessions of a deck-building task with escalating complexity (low and high), while ocular and cardiac activity and affective self-reports were recorded. We structure our discussion around three research questions: (1) assessing whether early ocular and cardiac signals are predictive of later performance outcomes as task complexity increases; (2) characterising the trajectories of physiological mechanisms reflected in key ocular and cardiac features that differentiate high- and low-performing groups across sessions; and (3) examining how subjective affective experiences performance outcomes diverge between these groups. We further consider broader implications of predictive ocular–cardiac signatures through two use cases that illustrate how these markers can be translated into human-state insights under demanding conditions.

7.1 RQ1: Ocular Signals and Multimodal Fusion Enable Early Prediction of Performance under Escalating Complexity

Addressing RQ1, our findings show that ocular features extracted from the early low-complexity session support the prospective prediction of later task performance. This finding extends performance-prediction research [35, 41, 107] by demonstrating that predictive information generalises across sessions in a continuously unfolding game environment. The early visual behaviour captured in

the low-complexity phase exhibited capability across individuals to support the forecasting of later outcomes. Multimodal fusion further improved performance, indicating that cardiac information contributed complementary signals not captured by ocular features alone.

The performance of the ocular-only model reflects the close coupling between visual sampling demands and task progress in our environment. Ablation analysis showed that its predictive value was driven by features describing where gaze was directed (AOI allocation) and how gaze shifted between elements (saccade dynamics). Their discriminative strength is consistent with prior work linking visual sampling behaviour to effective performance [14, 22, 83]. In addition, although the specific AOIs were derived from our game interface, gaze allocation to task-relevant regions has been widely used as a performance-related indicator in visually demanding interactions [33, 63, 83]. In our task, the interface is visually stable yet requires active information search given the strategic nature of the game. Accordingly, these predictors likely captured patterns of how gaze was allocated and distributed associated with performance outcomes. This suggests that ocular measures provide useful indicators for forecasting task performance, rather than merely describing viewing preferences.

On the other hand, pupillary features contributed less to early prediction. Although pupil diameter is a well-established indicator of arousal [38, 74] and cognitive control [118], its utility in the present task was likely constrained by dense, rapidly evolving in-game events. Prior work shows that pupil diameter increases during exploratory states and decreases during exploitation states

[38]. Participants may have experienced frequent event-evoked dilations and constrictions, producing oscillatory pupillary responses that weakened longer-term distinctions related to performance. In addition, frequent luminance variations within a visually dynamic game screen may have introduced light-evoked changes that further reduced discriminative power [8].

A parallel pattern emerged in the cardiac modality. Mean HR and HR range were the most predictive features, whereas HRV measures were weaker indicators in our task. Although HRV is typically associated with task-related regulation [19, 115] and has shown predictive value during high-intensity game events [66], it primarily reflects short-term autonomic modulation. In contrast, our turn-based task required sustained engagement over longer intervals rather than rapid, event-driven reactions. In this setting, overall levels of cardiac activation (HR) showed a stronger association with later performance, suggesting that tonic activation may offer more predictive value for cross-session prediction than momentary autonomic fluctuations.

Despite the lower unimodal accuracy of cardiac signals, the fused model achieved a more balanced class-wise performance by improving the identification of low-performing participants. This suggests that cardiac features encode discriminative information that is not fully captured in the ocular features and becomes useful particularly when the ocular classifier is uncertain. Additionally, the complementary value is localised to instances where the unimodal models diverge. As shown in the ablation analysis, training the meta-classifier on all samples caused the optimisation landscape to be dominated by majority agreement cases, which limited learning of decision rules from the informative disagreement region where cardiac signals add value. By restricting training to disagreement samples, the fused model was forced to learn from instances where the two modalities diverged, enabling it to exploit the complementary strength of cardiac information. This targeted integration produced the higher overall performance observed in the fused model.

7.2 RQ2: Ocular and Cardiac Signatures Reveal Divergent Visual Behaviours and Arousal Responses Across Performance Groups

Addressing RQ2, we identified two physiological patterns differentiating the performance groups across sessions: (1) how players visually accessed task-relevant information, reflected in saccade behaviour and gaze allocation; and (2) how physiological activation changed with increasing demands, reflected in heart-rate responses.

Gaze behaviour reflected clear differences in how players accessed task-relevant information. The high-performing group consistently allocated more gaze to strategically important interface elements throughout the task (potions and hand cards). Notably, the potion icons attracted sustained attention despite being located in peripheral regions. Such prioritisation has been widely associated with skilled viewing behaviour in visually demanding tasks [33, 63]. This aligns with the information-reduction perspective [36], which proposes that experienced performers concentrate processing on regions that are most useful for task progress. In our data, this translated into effective information access being established early and maintained throughout the task by the high-performing group.

Saccadic measures further revealed differences in how gaze shifts responded to increasing complexity. Early in the task, the high-performing group displayed both higher saccade rates and larger amplitudes, indicating that their gaze sampled more on-screen elements at this stage [90]. Interestingly, as complexity escalated, their amplitudes decreased while rates remained high, indicating a shift towards faster checks of relevant regions rather than broad scanning. This pattern reflects a transition from exploration to more compact sampling, consistent with task-driven viewing behaviours among skilled users reported in prior work [39, 61, 67]. This change was accompanied by a steady increase in the saccade-to-fixation ratio, showing that more gaze time remained devoted to sampling multiple elements as the task complexity increased [99]. In contrast, the low-performing group exhibited little change in sampling behaviour: scanning remained less active overall, and their saccade-to-fixation ratio stayed stable across sessions, indicating limited adjustment in how gaze time was distributed between movement and inspection. Notably, their amplitude increased only when demands intensified — a trend that moved in the opposite direction to the high-performing group. The late increase in amplitude may reflect the need to scan more widely distributed information once demands peaked, suggesting that the timing at which useful information was accessed became critical for task performance.

Heart rate reflected the extent to which task-evoked effort was sustained as demands increased. Within our study, HR rose for both groups when complexity escalated, a pattern consistent with prior observations that higher task demands are accompanied by elevated heart rate [3, 48]. Differences emerged most clearly in the high-complexity phase: the high-performing group showed a continued rise in HR, whereas the low-performing group plateaued. Prior work indicates that HR tends to increase when a task is experienced as demanding yet still attainable, whereas it stabilises when regulatory capacity is insufficient to meet rising demands [95, 96]. This suggests that maintaining elevated activation into the high-complexity phase appears more strongly associated with successful performance than initial reactivity alone, whereas stabilisation at a lower level coincided with poorer outcomes.

HR range further distinguished the groups. The low-performing group consistently exhibited larger HR ranges, indicating more variable cardiac activation. Such fluctuation suggests that their physiological state may have been more reactive to discrete in-game events (e.g., loss of HP or shifts in battle pace) [24]. These findings together reveal a non-linear cardiac response to escalating task complexity. In other words, what differentiated performance was not how high heart rate rose, but how reliably cardiac activation was maintained as demands escalated. Stable physiological mobilisation during the demanding phase appeared more consequential for eventual outcomes than initial reactivity alone.

Across ocular and cardiac channels, two hallmarks characterised successful performance in our study: (1) sustained visual attention towards task-relevant areas, accompanied by timely gaze shifts as complexity increased, and (2) stable cardiac activation when demands intensified. Participants who showed both continued to access useful information and maintained the activation needed to act upon it under high demands, whereas others either did not prioritise relevant information sufficiently or exhibited less stable activation in the most demanding phase. These physiological

patterns provide interpretable indicators of how information was accessed and how effort was sustained across escalating task demands.

7.3 RQ3: Divergent Affective Trajectories and Sense of Control Across Performance Groups

Addressing RQ3, we found participants' affective responses to escalating task demands diverged by performance group, particularly in valence and dominance, despite similar increases in arousal and perceived difficulty. Across high- and low-performing groups, participants consistently reported greater perceived difficulty in the high-complexity stage, confirming that task complexity was effectively manipulated by the natural game progression, as reflected in the rise of arousal during the high-complexity session in both groups. Yet their affective trajectories diverged. Among high-performing participants, elevated arousal was accompanied by higher positive valence, a pattern consistent with Self-Determination Theory and flow theory [97, 110], where arousal induced by optimal challenge sustains positive affect, provided that competence is preserved. Notably, even in the early stage, low-performing participants already reported more negative emotions (see Figure 8), suggesting that limited familiarity or weaker perceived control of the game mechanics caused confusion or disengagement from the outset.

This lack of differentiation in overall affective arousal provides interpretative context for our prediction model results: physiological features that are associated with general arousal level (e.g., HR and Pupil) show limited discriminative power for performance prediction, as high arousal was a common state across participants in our context. At the same time, low-performing participants showed a stronger increase in arousal from low to high complexity, indicating greater sensitivity to task demand escalation. These patterns suggest that the way arousal changes with task demands may be more informative for distinguishing performance trajectories than the absolute arousal state itself.

Dominance trajectories also diverged between high- and low-performing groups. As complexity rose, reported dominance declined for all participants, but the high-performing group reported less erosion of dominance. For the low-performing group, the same failure situation led to divergent dominance experiences, as evidenced by the more polarised distribution. This variability suggests that low-performing participants did not interpret the failure state uniformly: while some retained a sense of agency, others experienced a marked collapse of control [11, 51, 52]. Dominance therefore complements arousal by characterising how players construe difficulty, rather than how intensely they react to it. This affective dimension reveals distinct psychological pathways into failure that are not evident from physiological responses alone.

7.4 Broader Implications: From predictive signatures to Human-State Insights

Within a single game context, the observed ocular and cardiac patterns demonstrate the potential of physiological patterns to inform interpretable characterisations of human state under increasing task demands. Our model shows that early ocular-cardiac patterns can

forecast later performance under escalating complexity: fewer saccades and a narrower scan range (Fig. 14 C, D, E), and reduced gaze distribution over the critical AOI (Fig. 14 A, B) were characteristic of at-risk trajectories, whereas high-performing participants exhibited broader and more frequent saccades and allocated gaze more consistently toward task-relevant elements. Cardiac signals further showed that high-performing participants maintained higher HR throughout (Fig. 12A), whereas the low-performing group exhibited a consistently larger HR range (Fig. 12B). These multimodal signatures provide early markers of visual strategies and physiological activation that precede measurable differences in performance.

Use case 1 – Early signatures of limited visual sampling. In the initial phase of tasks, saccadic and gaze allocation patterns associated with proactive visual behaviour can serve as measurable indicators of emerging strain. Lower saccade rates, narrow saccade amplitudes, and limited gaze on critical regions indicate a lack of proactive information sampling, where access to task-relevant cues becomes more delayed or less frequent. These signatures delineate a window in which suboptimal allocation of visual attention and information scanning emerges before observable differences in performance, particularly in visually intensive tasks with a relatively stable interface structure. Early detection of these patterns could inform design approaches to scaffolding or information guidance in contexts where sustaining focus on task-relevant elements is critical, for instance redirecting visual attention towards elements that most strongly support task progress.

Use case 2 – Phase-transition markers. At natural transitions in task structure, such as shifts from low to high workload, cardiac measures provide early indicators of how well physiological activation is being sustained. A plateau in HR across a transition suggests that mobilisation is not increasing in line with escalating demands, while a larger HR range indicates more reactive, event-driven fluctuations. These features reveal moments when activation becomes less stable under pressure, offering a physiological lens on when individuals may be more vulnerable to errors. These markers could support strategic pauses or checkpoint-guided interventions in domains such as training, education, and safety-critical operations, where phase transitions are central to task structure.

7.5 Limitations and Future Work

Our study was conducted in a single game, *Slay the Spire*, which provided a progressively challenging and ecologically valid environment for testing predictive physiology. However, this setting emphasises individual decision-making and turn-based strategy. This limitation is particularly relevant for ocular measures, which are known to be highly sensitive to task structure and visual layout. Consequently, the predictive value of eye-movement features observed in this study should be interpreted as context-specific. Future work should evaluate whether the same multimodal patterns emerge in broader interactive contexts that place different demands on users, such as sustained collaboration or safety-critical training tasks. Examining these varied settings would help establish the boundary conditions of physiological forecasting and determine how robustly ocular and cardiac signals generalise across domains.

A second limitation concerns the heterogeneity observed within the loss group. Performance outcome (high-performing vs. low-performing) served as the most robust and interpretable indicator of performance, yet our analysis of self-reported dominance showed marked variation among participants. Some retained a sense of control despite losing, whereas others experienced a complete collapse of agency. This suggests that the binary outcome may obscure distinct failure pathways. Future research should distinguish subtypes of low-performing participants, for example by clustering physiological and experiential profiles within the low-performing group and incorporating additional evaluative elements, thereby capturing how different breakdown trajectories manifest in both signals and experience.

A third limitation concerns the cardiac data acquisition. We utilised a wrist-worn PPG device sampling at 64 Hz, selected for its lightweight design and minimal disruption during gameplay. While this sampling rate is sufficient for heart-rate estimation, it lacks the temporal resolution required for reliable short-term HRV computation, where millisecond-level precision is necessary for capturing beat-to-beat variation. Although the inter-beat intervals were stabilised through interpolation, the HRV-derived features did not improve predictive performance. It therefore remains an open question whether higher-fidelity sensors would yield more informative HRV measures in this task context. As HRV is the most informative component of cardiac activity for inferring autonomic regulation, future work would benefit from incorporating higher-fidelity sensors or ECG-based systems to obtain more reliable HRV and allow a clearer assessment of its predictive value.

A fourth limitation concerns the absence of a pre-task physiological baseline. The study began with the gameplay sequence; although within-subject z-score normalisation reduced intra-individual variability, this procedure cannot recover information about participants' tonic arousal or pre-existing anxiety levels prior to task onset. These baseline traits influence both pupil-linked arousal and autonomic cardiac reactivity and therefore impose an unknown offset on the subsequent task-evoked responses. Without a dedicated resting phase, it is difficult to determine whether observed physiological differences reflect genuine task-induced regulation or underlying stable traits. Future protocols incorporating a controlled resting baseline would enable clearer separation of task-evoked dynamics from individual physiological predispositions and improve interpretability of anticipatory physiological markers.

Finally, our modelling was validated in a relatively small participant cohort. Given the exploratory nature of this study, future work with larger and more diverse samples will be important for assessing the generalisability of current findings.

8 Conclusions

This study examined whether early ocular and cardiac signals can prospectively predict later performance outcomes as task complexity increases in a game environment. A within-subject experiment with 35 participants was conducted, combining ocular and cardiac measurements with self-reported affective ratings. We evaluated the predictive power of ocular, cardiac, and decision-level fused models under a LOSO cross-subject validation protocol. Beyond prediction, we analysed group-level feature trends across complexity

phases and subjective affective reports to contextualise performance differences in relation to physiological dynamics and subjective appraisal.

In response to RQ1, ocular features and the fused model effectively predicted later performance, whereas the cardiac model alone was weaker. Across modalities, gaze distribution, saccade behaviour, and heart rate were the main predictive features. For RQ2, high-performing participants maintained targeted gaze on task-relevant elements, timely adapted their visual sampling as demands increased, and sustained more stable cardiac activation into the high-complexity phase, indicating distinct visual behaviour and autonomic mobilisation under pressure. For RQ3, the high-performing group reported more positive affective experience, while the low-performing group displayed a wider spread in their reported sense of control.

In the future, we will extend this work to examine whether the physiological signatures observed in the present task generalise to broader interactive contexts, particularly those involving complex task dynamics and phase transitions. Further research will also explore heterogeneity within low-performing participants by identifying subtypes of failure trajectories through clustering of physiological and experiential profiles. In addition, using higher-sampling-rate sensors for HRV estimation would provide more reliable autonomic markers and allow a more precise characterisation of cardiac contributions to performance prediction. By addressing these directions, future work can extend beyond the current task setting and build multimodal indicators that support predictive systems capable of anticipating performance breakdowns, while advancing quantitative insight into how user states evolve under escalating task complexity.

References

- [1] Gökhan Akçapınar, Arif Altun, and Petek Aşkar. 2019. Using learning analytics to develop early-warning system for at-risk students. *International Journal of Educational Technology in Higher Education* 16, 1 (2019), 1–20.
- [2] Samuel Almeida, Oscar Mealha, and Ana Veloso. 2016. Video Game Scenery Analysis with Eye Tracking. *Entertainment Computing* 16 (2016), 35–44. doi:10.1016/j.entcom.2016.03.002
- [3] Evgeniia I Alshanskaia, Natalia A Zhzhikhshvili, Irina S Polikanova, and Olga V Martynova. 2024. Heart rate response to cognitive load as a marker of depression and increased anxiety. *Frontiers in Psychiatry* 15 (2024), 1355846.
- [4] Omar A Alzubi, Jafar Ahmad Abed Alzubi, Sara Tedmori, Hasan Rashaideh, and Omar Almomani. 2018. Consensus-based combining method for classifier ensembles. *Int. Arab J. Inf. Technol.* 15, 1 (2018), 76–86.
- [5] Zahra Azizah, Tomoya Ohyama, Xiumin Zhao, Yuichi Ohkawa, and Takashi Mitsuishi. 2024. Predicting at-risk students in the early stage of a blended learning course via machine learning using limited data. *Computers and Education: Artificial Intelligence* 7 (2024), 100261.
- [6] Dinko Bačić and Raymond Henry. 2022. Advancing our understanding and assessment of cognitive effort in the cognitive fit theory and data visualization context: Eye tracking-based approach. *Decision Support Systems* 163 (2022), 113862.
- [7] Hyoung Joon Baek, Chi Ho Cho, Jaeuk Cho, and Jong Min Woo. 2015. Reliability of ultra-short-term analysis as a surrogate of standard 5-min analysis of heart rate variability. *Telemedicine and e-Health* 21, 5 (2015), 404–414.
- [8] Jackson Beatty and Brennis Lucero-Wagoner. 2000. The pupillary system. In *Handbook of psychophysiology* (2 ed.), John T Cacioppo, Louis G Tassinary, and Gary G Berntson (Eds.). Cambridge University Press, Cambridge, 142–162.
- [9] Mahnaz Behroozi, Alison Lui, Ian Moore, Denae Ford, and Chris Parnin. 2018. Dazed: measuring the cognitive load of solving technical interview problems at the whiteboard. In *Proceedings of the 40th international conference on software engineering: New Ideas and Emerging Results*. 93–96.
- [10] Bartosz Binias, Dariusz Myszor, Henryk Palus, and Krzysztof A Cyran. 2020. Prediction of pilot's reaction time based on EEG signals. *Frontiers in neuroinformatics* 14 (2020), 6.

- [11] Julia Ayumi Bopp, Elisa D Mekler, and Klaus Opwis. 2016. Negative emotion, positive experience? Emotionally moving moments in digital games. In *Proceedings of the 2016 CHI conference on human factors in computing systems*. 2996–3006.
- [12] Marie-Line Bosse, Marie Joséphe Tainturier, and Sylviane Valdois. 2007. Developmental dyslexia: The visual attention span deficit hypothesis. *Cognition* 104, 2 (2007), 198–230.
- [13] Gary Bradski. 2000. The OpenCV Library. *Dr. Dobb's Journal of Software Tools* (2000).
- [14] Stephanie Brams, Gal Ziv, Oron Levin, Jochim Spitz, Johan Wagemans, A Mark Williams, and Werner F Helsen. 2019. The relationship between gaze behavior, expertise, and performance: A systematic review. *Psychological bulletin* 145, 10 (2019), 980.
- [15] John T Cacioppo, Louis G Tassinary, and Gary Berntson. 2007. *Handbook of psychophysiology*. Cambridge university press.
- [16] John P. Campbell. 1990. Modeling the performance prediction problem in industrial and organizational psychology. In *Handbook of Industrial and Organizational Psychology*, Marvin D. Dunnette and Leaetta M. Hough (Eds.). Vol. 1. Consulting Psychologists Press, Palo Alto, CA, 687–732.
- [17] Genís Cardona and Noa Quevedo. 2014. Blinking and driving: the influence of saccades and cognitive workload. *Current eye research* 39, 3 (2014), 239–244.
- [18] Tianqi Chen and Carlos Guestrin. 2016. XGBoost: A Scalable Tree Boosting System. In *Proceedings of the 22nd ACM SIGKDD International Conference on Knowledge Discovery and Data Mining*. 785–794. doi:10.1145/2939672.2939785
- [19] Lorenza S Colzato, Bryant J Jongkees, Matthijs de Wit, Melle JW van der Molen, and Laura Steenbergen. 2018. Variable heart rate and a flexible mind: Higher resting-state heart rate variability predicts better task-switching. *Cognitive, Affective, & Behavioral Neuroscience* 18 (2018), 730–738.
- [20] William J. Conover. 1999. *Practical Nonparametric Statistics* (3 ed.). John Wiley & Sons, New York.
- [21] Corinna Cortes and Vladimir Vapnik. 1995. Support Vector Networks. *Machine Learning* 20, 3 (1995), 273–297. doi:10.1007/BF00994018
- [22] Berrin Dogusoy-Taylan and Kursat Cagiltay. 2014. Cognitive analysis of experts' and novices' concept mapping processes: An eye tracking study. *Computers in human behavior* 36 (2014), 82–93.
- [23] Kevin Doherty and Gavin Doherty. 2018. Engagement in HCI: Conception, Theory and Measurement. *Comput. Surveys* 51, 5, Article 100 (2018). doi:10.1145/3234149
- [24] Anders Drachen, Lennart E Nacke, Georgios Yannakakis, and Anja Lee Pedersen. 2010. Correlation between heart rate, electrodermal activity and player experience in first-person shooter games. In *Proceedings of the 5th ACM SIGGRAPH Symposium on Video Games*. 49–54.
- [25] Ke-Lin Du, Rengong Zhang, Bingchun Jiang, Jie Zeng, and Jiabin Lu. 2025. Foundations and innovations in data fusion and ensemble learning for effective consensus. *Mathematics* 13, 4 (2025), 587.
- [26] Dennis E Egan. 1988. Individual differences in human-computer interaction. In *Handbook of human-computer interaction*. Elsevier, 543–568.
- [27] Empatica Inc. 2025. EmbracePlus: Multisensor Wearable Device. <https://www.empatica.com/embraceplus>. Empatica Inc., Milan, Italy. Accessed: 2025-09-07.
- [28] Mica R. Endsley. 1997. The role of situation awareness in naturalistic decision making. In *Naturalistic Decision Making*, Caroline E. Zsombok and Gary Klein (Eds.). Lawrence Erlbaum Associates, Mahwah, NJ, 269–283.
- [29] Ralf Engbert, Hans A Trukenbrod, Simon Barthelmé, and Felix A Wichmann. 2015. Spatial statistics and attentional dynamics in scene viewing. *Journal of vision* 15, 1 (2015), 14–14.
- [30] Tjitske JE Faber, Mary EW Dankbaar, Walter W van den Broek, Laura J Bruinink, Marije Hogeveen, and Jeroen JG van Merriënboer. 2024. Effects of adaptive scaffolding on performance, cognitive load and engagement in game-based learning: a randomized controlled trial. *BMC Medical Education* 24, 1 (2024), 943.
- [31] Borna Fatehi, Casper Harteveld, and Christoffer Holmgård. 2022. Guiding Game Design Decisions via Eye-Tracking: An Indie Game Case Study. In *2022 Symposium on Eye Tracking Research and Applications*. 1–7.
- [32] John M Findlay. 1997. Saccade target selection during visual search. *Vision research* 37, 5 (1997), 617–631.
- [33] F. Fogarty et al. 2023. Eye tracking in surgical performance assessment: A systematic review. *Surgical Endoscopy* 37 (2023), 1234–1247. doi:10.1007/s00464-022-09667-0
- [34] Rahul Gavas, Debatri Chatterjee, and Aniruddha Sinha. 2017. Estimation of cognitive load based on the pupil size dilation. In *2017 IEEE international conference on systems, man, and cybernetics (SMC)*. IEEE, 1499–1504.
- [35] Hao Guo, Wei Fan, Shaohui Liu, Feng Jiang, and Chunzhi Yi. 2025. PPTP: Performance-Guided Physiological-Signal-Based Trust Prediction in Human-Robot Collaboration. arXiv preprint arXiv:2506.16677. Submitted 20 June 2025.
- [36] Hilde Haider and Peter A. Frensch. 1999. Eye movement during skill acquisition: More evidence for the information-reduction hypothesis. *Journal of Experimental Psychology: Learning, Memory, and Cognition* 25, 1 (1999), 172–190. doi:10.1037/0278-7393.25.1.172
- [37] Anita Lill Hansen, Bjørn Helge Johnsen, and Julian F. Thayer. 2003. Vagal influence on working memory and attention. *International Journal of Psychophysiology* 48, 3 (2003), 263–274. doi:10.1016/S0167-8760(03)00073-4
- [38] Taylor R Hayes and Alexander A Petrov. 2016. Pupil diameter tracks the exploration–exploitation trade-off during analogical reasoning and explains individual differences in fluid intelligence. *Journal of cognitive neuroscience* 28, 2 (2016), 308–318.
- [39] Mary Hayhoe and Dana Ballard. 2005. Eye movements in natural behavior. *Trends in Cognitive Sciences* 9, 4 (2005), 188–194. doi:10.1016/j.tics.2005.02.009
- [40] Jennifer A Healey and Rosalind W Picard. 2005. Detecting stress during real-world driving tasks using physiological sensors. *IEEE Transactions on intelligent transportation systems* 6, 2 (2005), 156–166.
- [41] Jamison Heard, Prakash Baskaran, and Julie A. Adams. 2022. Predicting Task Performance for Intelligent Human-Machine Interactions. *Frontiers in Neurorobotics* 16 (2022), 973967. doi:10.3389/fnbot.2022.973967
- [42] Calum Hennings, Muneeb Ahmad, and Katrin Lohan. 2021. Real-Time Adaptive Game to Reduce Cognitive Load. In *Proceedings of the 9th International Conference on Human-Agent Interaction (Virtual Event, Japan) (HAI '21)*. Association for Computing Machinery, New York, NY, USA, 342–347. doi:10.1145/3472307.3484674
- [43] Eckhard H. Hess and James M. Polt. 1960. Pupil size as related to interest value of visual stimuli. *Science* 132, 3423 (1960), 349–350. doi:10.1126/science.132.3423.349
- [44] Kenneth Holmqvist, Marcus Nyström, Richard Andersson, Richard Dewhurst, Halszka Jarodzka, and Joost van de Weijer. 2011. *Eye Tracking: A Comprehensive Guide to Methods and Measures*. Oxford University Press, Oxford, UK. doi:10.1093/acprof:oso/9780199697083.001.0001
- [45] Edward H. Hon and Steven T. Lee. 1965. Electronic evaluations of the fetal heart rate patterns preceding fetal death: further observations. *American Journal of Obstetrics and Gynecology* 87, 6 (1965), 814–826.
- [46] Samuel B Hutton. 2008. Cognitive control of saccadic eye movements. *Brain and cognition* 68, 3 (2008), 327–340.
- [47] International Organization for Standardization. 2018. Ergonomics of human-system interaction – Part 11: Usability: Definitions and concepts. ISO 9241-11:2018. <https://www.iso.org/standard/63500.html>
- [48] Petar Jerčić, Charlotte Sennersten, and Craig Lindley. 2020. Modeling cognitive load and physiological arousal through pupil diameter and heart rate. *Multimedia Tools and Applications* 79, 5 (2020), 3145–3159.
- [49] PGAM Jorna. 1993. Heart rate and workload variations in actual and simulated flight. *Ergonomics* 36, 9 (1993), 1043–1054.
- [50] Marcel A. Just and Patricia A. Carpenter. 1976. Eye fixations and cognitive processes. *Cognitive Psychology* 8, 4 (1976), 441–480. doi:10.1016/0010-0285(76)90015-3
- [51] Jesper Juul. 2013. *The art of failure: An essay on the pain of playing video games*. MIT press.
- [52] Manu Kapur. 2016. Examining productive failure, productive success, unproductive failure, and unproductive success in learning. *Instructional Science* 44, 4 (2016), 451–465. doi:10.1007/s11251-016-9379-6
- [53] David O Kennedy and Andrew B Scholey. 2000. Glucose administration, heart rate and cognitive performance: effects of increasing mental effort. *Psychopharmacology* 149 (2000), 63–71.
- [54] Kristian Kiili, Harri Ketamo, and Michael D. Kickmeier-Rust. 2014. Eye Tracking in Game-based Learning Research and Game Design. *International Journal of Serious Games* 1, 2 (2014), 51–65. doi:10.17083/ijsg.v1i2.15
- [55] Josef Kittler, Mohamad Hatf, Robert PW Duin, and Jiri Matas. 2002. On combining classifiers. *IEEE transactions on pattern analysis and machine intelligence* 20, 3 (2002), 226–239.
- [56] Peter König, Niklas Wilming, Tim C Kietzmann, Jose P Ossandón, Selim Onat, Benedikt V Ehinger, Ricardo R Gameiro, and Kai Kaspar. 2016. Eye movements as a window to cognitive processes. *Journal of eye movement research* 9, 5 (2016), 25.
- [57] Estela Kristal-Boneh, Mark Raifel, Paul Froom, and Joseph Ribak. 1995. Heart rate variability in health and disease. *Scandinavian journal of work, environment & health* (1995), 85–95.
- [58] Sylvain Laborde, Markus Raab, and Nannie P Kinrade. 2014. Is the ability to keep your mind on the game related to heart rate variability? *Sport, Exercise, and Performance Psychology* 3, 4 (2014), 285–297.
- [59] Dana Lahat, Tülay Adalı, and Christian Jutten. 2015. Multimodal data fusion: an overview of methods, challenges, and prospects. *Proc. IEEE* 103, 9 (2015), 1449–1477.
- [60] Xuan Lan, Lei Duan, Wen Chen, Ruiqi Qin, Timo Nummenmaa, and Jyrki Nummenmaa. 2018. A player behavior model for predicting win-loss outcome in MOBA games. In *International Conference on Advanced Data Mining and Applications*. Springer, 474–488.
- [61] Michael F. Land and Benjamin W. Tatler. 2006. *Looking and Acting: Vision and Eye Movements in Natural Behaviour*. Oxford University Press, Oxford, UK. doi:10.1093/acprof:oso/9780198570943.001.0001
- [62] Boyi Li, Tsubasa Minematsu, Yuta Taniguchi, Fumiyo Okubo, and Atsushi Shimada. 2022. How Does Analysis of Handwritten Notes Provide Better Insights

- for Learning Behavior?. In *Proceedings of the 12th International Conference on Learning Analytics and Knowledge (LAK '22)*. Association for Computing Machinery, 549–555. doi:10.1145/3506860.3506915
- [63] Shan Li, Melissa C Duffy, Susanne P Lajoie, Juan Zheng, and Kevin Lachapelle. 2023. Using eye tracking to examine expert-novice differences during simulated surgical training: A case study. *Computers in Human Behavior* 144 (2023), 107720.
- [64] W. L. Libby, B. C. Lacey, and J. I. Lacey. 1973. Pupillary and cardiac activity during visual attention. *Psychophysiology* 10, 3 (1973), 270–294. doi:10.1111/j.1469-8986.1973.tb00526.x
- [65] Simon P Liversedge and John M Findlay. 2000. Saccadic eye movements and cognition. *Trends in cognitive sciences* 4, 1 (2000), 6–14.
- [66] Kehong Long, Xuzhe Zhang, Ningxin Wang, and Hao Lei. 2023. Heart Rate Variability during Online Video Game Playing in Habitual Gamers: Effects of Internet Addiction Scale, Ranking Score and Gaming Performance. *Brain Sciences* 14, 1 (2023), 29.
- [67] Wenyi Lu, Hao He, Alex Urban, and Joe Griffin. 2021. What the eyes can tell: Analyzing visual attention with an educational video game. In *ACM Symposium on Eye Tracking Research and Applications*. 1–7.
- [68] Yifei Lu, Wei-Long Zheng, Binbin Li, and Bao-Liang Lu. 2015. Combining eye movements and EEG to enhance emotion recognition. In *Proceedings of the 24th International Conference on Artificial Intelligence (IJCAI'15)*. AAAI Press, 1170–1176.
- [69] Antonio Luque-Casado, José C Perales, David Cárdenas, and Daniel Sanabria. 2016. Heart rate variability and cognitive processing: The autonomic response to task demands. *Biological psychology* 113 (2016), 83–90.
- [70] G Luzzani, I Buraoli, D Demarchi, and G Guglieri. 2024. A review of physiological measures for mental workload assessment in aviation: A state-of-the-art review of mental workload physiological assessment methods in human-machine interaction analysis. *The Aeronautical Journal* 128, 1323 (2024), 928–949.
- [71] Arien Mack. 2003. Inattentive blindness: Looking without seeing. *Current directions in psychological science* 12, 5 (2003), 180–184.
- [72] Dominique Makowski, Tam Pham, Zen J Lau, Jan C Brammer, François Lespinasse, Hung Pham, Christopher Schölzel, and SH Annabel Chen. 2021. NeuroKit2: A Python toolbox for neurophysiological signal processing. *Behavior research methods* (2021), 1–8.
- [73] Rohit Mallick, David Slayback, Jon Touryan, Anthony J Ries, and Brent J Lance. 2016. The use of eye metrics to index cognitive workload in video games. In *2016 IEEE second workshop on eye tracking and visualization (etvis)*. IEEE, 60–64.
- [74] Sandra P Marshall. 2007. Identifying cognitive state from eye metrics. *Aviation, Space, and Environmental Medicine* 78, 5 (2007), B165–B175.
- [75] MegaCrit. 2017. Slay the Spire. Video Game, Available on PC, PlayStation 4, Xbox One, Nintendo Switch.
- [76] B. Mehler, B. Reimer, and J. F. Coughlin. 2012. Sensitivity of physiological measures for detecting systematic variations in cognitive demand from a working memory task: An on-road study across three age groups. *Human Factors* 54, 3 (2012), 396–412. doi:10.1177/0018720812446433
- [77] Elisa D. Mekler, Florian Brühlmann, Klaus Opwis, and Alexandre N. Tuch. 2013. Measuring the effect of gamification: the role of motivation and performance. In *Proceedings of the SIGCHI Conference on Human Factors in Computing Systems (CHI '13 Extended Abstracts)*. ACM, 1039–1042. doi:10.1145/2468356.2468559
- [78] Elisa D. Mekler, Florian Brühlmann, Alexandre N. Tuch, and Klaus Opwis. 2017. Towards understanding the effects of individual gamification elements on intrinsic motivation and performance. In *Proceedings of the 2017 CHI Conference on Human Factors in Computing Systems (CHI '17)*. ACM, 5117–5129. doi:10.1145/3025453.3025982
- [79] Sorato Minami, Haruki Koyama, Ken Watanabe, Naoki Saijo, and Makio Kashino. 2024. Prediction of esports competition outcomes using EEG data from expert players. *Computers in Human Behavior* 160 (2024), 108351.
- [80] Maria L Munoz, Arie van Roon, Harriëtte Riese, Chris Thio, Esther Oostenbroek, Ilse Westrik, Eco J. C. de Geus, Ron T. Gansevoort, Joop D. Lefrandt, Ilja M. Nolte, and Harold Snieder. 2015. Validity of (ultra-) short recordings for heart rate variability measurements. *PloS one* 10, 9 (2015), e0138921.
- [81] Lennart E. Nacke and Sebastian Deterding. 2017. The maturing of gamification research. *Computers in Human Behavior* 71 (2017), 450–454. doi:10.1016/j.chb.2016.11.062
- [82] Shivsevak Negi and Ritayan Mitra. 2020. Fixation duration and the learning process: An eye tracking study with subtitled videos. *Journal of Eye Movement Research* 13, 6 (2020), 1–15.
- [83] Kristien Ooms, Philippe De Maeyer, and Veerle Fack. 2014. Study of the attentive behavior of novice and expert map users using eye tracking. *The Cartographic Journal* 51, 4 (2014), 339–350.
- [84] Gyeong Park, Michael W. Vasey, Jay J. Van Bavel, and Julian F. Thayer. 2014. Resting heart rate variability is associated with cognitive flexibility in older adults: The moderating role of age. *Psychophysiology* 51, 5 (2014), 466–475. doi:10.1111/psyp.12191
- [85] Edward J Peacock and Paul TP Wong. 1990. The stress appraisal measure (SAM): A multidimensional approach to cognitive appraisal. *Stress medicine* 6, 3 (1990), 227–236.
- [86] Roxy Peck, Chris Olsen, and Jay L. Devore. 2015. *Introduction to Statistics and Data Analysis* (5 ed.). Cengage Learning, Boston, MA.
- [87] Jonathan E Peelle and Kristin J Van Engen. 2021. Time stand still: Effects of temporal window selection on eye tracking analysis. *Collabra: Psychology* 7, 1 (2021), 25961.
- [88] Vsevolod Peysakhovich, Frédéric Dehais, and Mickaël Causse. 2015. Pupil diameter as a measure of cognitive load during auditory-visual interference in a simple piloting task. *Procedia Manufacturing* 3 (2015), 5199–5205.
- [89] Tam Pham, Zen Juen Lau, SH Annabel Chen, and Dominique Makowski. 2021. Heart rate variability in psychology: A review of HRV indices and an analysis tutorial. *Sensors* 21, 12 (2021), 3998.
- [90] Matthew H Phillips and Jay A Edelman. 2008. The dependence of visual scanning performance on saccade, fixation, and perceptual metrics. *Vision research* 48, 7 (2008), 926–936.
- [91] Alex Poole and Linden J. Ball. 2006. Eye Tracking in Human-Computer Interaction and Usability Research: Current Status and Future Prospects. In *Encyclopedia of Human-Computer Interaction*, Claude Ghaoui (Ed.). IGI Global, 211–219. doi:10.4018/978-1-59140-562-7.ch034
- [92] Annu Pradhan and Ela Kumar. 2022. Cognitive workload estimation using eye tracking: a review. In *International Conference on Advancements in Interdisciplinary Research*. Springer, 544–552.
- [93] Ludmila Prokhorenkova, Gleb Gusev, Aleksandr Vorobei, Anna Veronika Dorogush, and Andrey Gulin. 2018. CatBoost: Unbiased Boosting with Categorical Features. In *Advances in Neural Information Processing Systems*.
- [94] Keith Rayner. 1978. Eye movements in reading and information processing. *Psychological bulletin* 85, 3 (1978), 618.
- [95] Michael Richter, Antonia Friedrich, and Guido HE Gendolla. 2008. Task difficulty effects on cardiac activity. *Psychophysiology* 45, 5 (2008), 869–875.
- [96] M Richter, GHE Gendolla, and RA Wright. 2016. Three decades of research on motivational intensity theory: What we have learned about effort and what we still don't know. *Advances in motivation science* 3 (2016), 149–186.
- [97] Richard M. Ryan and Edward L. Deci. 2017. *Self-Determination Theory: Basic Psychological Needs in Motivation, Development, and Wellness*. The Guilford Press, New York, NY.
- [98] Mazen Salous, Felix Putze, Tanja Schultz, Jutta Hild, and Jürgen Beyerer. 2018. Investigating static and sequential models for intervention-free selection using multimodal data of EEG and eye tracking. In *Proceedings of the Workshop on Modeling Cognitive Processes from Multimodal Data*. 1–6.
- [99] Dario D Salvucci and Joseph H Goldberg. 2000. Identifying fixations and saccades in eye-tracking protocols. In *Proceedings of the 2000 symposium on Eye tracking research & applications*. 71–78.
- [100] Marko Sarlija et al. 2020. Prediction of task performance from physiological features of stress resilience. *IEEE Journal of Biomedical and Health Informatics* 24, 12 (2020), 3456–3465.
- [101] Abraham Savitzky and Marcel J. E. Golay. 1964. Smoothing and Differentiation of Data by Simplified Least Squares Procedures. *Analytical Chemistry* 36, 8 (1964), 1627–1639. doi:10.1021/ac60214a047
- [102] Ceyda Sayali, Emma Heling, and Roshan Cools. 2023. Learning progress mediates the link between cognitive effort and task engagement. *Cognition* 236 (2023), 105418.
- [103] Magali Seassau, Christophe Loic Gérard, Emmanuel Bui-Quoc, and Maria Pia Bucci. 2014. Binocular saccade coordination in reading and visual search: a developmental study in typical reader and dyslexic children. *Frontiers in integrative neuroscience* 8 (2014), 85.
- [104] Ben Shneiderman. 1979. Human factors experiments in designing interactive systems. *Computer* 12, 12 (1979), 9–19.
- [105] Ciara Sibley, Joseph Coyne, and Carryl Baldwin. 2011. Pupil dilation as an index of learning. In *Proceedings of the Human Factors and Ergonomics Society Annual Meeting*, Vol. 55. SAGE Publications Sage CA: Los Angeles, CA, 237–241.
- [106] George Siemens and Ryan S. J. d. Baker. 2012. Learning analytics and educational data mining: Towards communication and collaboration. *Proceedings of the 2nd International Conference on Learning Analytics and Knowledge* (2012), 252–254. doi:10.1145/2330601.2330661
- [107] Anton Smerdov, Andrey Somov, Evgeny Burnaev, and Anton Stepanov. 2023. AI-enabled prediction of video game player performance using the data from heterogeneous sensors. *Multimedia Tools and Applications* 82, 7 (2023), 11021–11046.
- [108] Andreas Sonderegger and Juergen Sauer. 2010. The influence of design aesthetics in usability testing: Effects on user performance and perceived usability. *Applied ergonomics* 41, 3 (2010), 403–410.
- [109] H. Stemmann and W.A. Freiwald. 2010. Attentional modulation of visual processing. *Neuron* 67, 5 (2010), 927–939.
- [110] Penelope Sweetser and Peta Wyeth. 2005. GameFlow: a model for evaluating player enjoyment in games. *Computers in Entertainment (CIE)* 3, 3 (2005), 3–3.
- [111] John Sweller. 1994. Cognitive load theory, learning difficulty, and instructional design. *Learning and instruction* 4, 4 (1994), 295–312.

- [112] Task Force of the European Society of Cardiology and the North American Society of Pacing and Electrophysiology. 1996. Heart rate variability: standards of measurement, physiological interpretation and clinical use. *Circulation* 93, 5 (1996), 1043–1065.
- [113] Benjamin W Tatler, Mary M Hayhoe, Michael F Land, and Dana H Ballard. 2017. Eye movements and the control of attention in natural scenes. *Philosophical Transactions of the Royal Society B: Biological Sciences* 372, 1711 (2017), 20160106.
- [114] NeuroKit Development Team. 2024. NeuroKit: A Python Toolbox for Statistics and Signal Processing of Biological Data. <https://github.com/neuropsychology/NeuroKit> Accessed: 2024-08-12.
- [115] Julian F. Thayer, Asmund L. Hansen, Even Saus-Rose, and Bjørn H. Johnsen. 2009. Heart rate variability, prefrontal neural function, and cognitive performance: The neurovisceral integration perspective. *Psychological Science* 20, 12 (2009), 141–146. doi:10.1111/j.1467-9280.2009.02473.x
- [116] Tobii AB. 2019. Tobii Pro Fusion Eye Tracker. <https://www.tobii.com/products/eye-trackers/screen-based/tobii-pro-fusion>. Accessed: 2025-09-10.
- [117] Tobii Technology AB. 2023. Let's talk accuracy and precision. <https://help.tobii.com/hc/en-us/articles/213534825-Let-s-talk-accuracy-and-precision> Accessed: 2025-09-07.
- [118] Pauline Van der Wel and Henk Van Steenbergen. 2018. Pupil dilation as an index of effort in cognitive control tasks: A review. *Psychonomic bulletin & review* 25, 6 (2018), 2005–2015.
- [119] Boris B Velichkovsky, Nikita Khromov, Alexander Korotin, Evgeny Burnaev, and Andrey Somov. 2019. Visual fixations duration as an indicator of skill level in esports. In *Human-Computer Interaction—INTERACT 2019: 17th IFIP TC 13 International Conference, Paphos, Cyprus, September 2–6, 2019, Proceedings, Part I 17*. Springer, 397–405.
- [120] Kaiqi Wei, Chika Kimura, Megumi Shimura, Yoshihiro Shimomura, Xue Zhao, Takaaki Tamura, and Shinichi Sakamoto. 2025. Predicting task performance in robot-assisted surgery using physiological stress and subjective workload: a case study with interpretable machine learning. *Frontiers in Human Neuroscience* 19 (2025), 1611524.
- [121] Philip H. Winne and Nancy E. Perry. 2000. Measuring self-regulated learning. In *Handbook of Self-Regulation*, Monique Boekaerts, Paul R. Pintrich, and Moshe Zeidner (Eds.). Academic Press, 531–566.
- [122] Christian Wolf and Markus Lappe. 2021. Vision as oculomotor reward: cognitive contributions to the dynamic control of saccadic eye movements. *Cognitive Neurodynamics* 15, 4 (2021), 547–568.
- [123] David H Wolpert. 1992. Stacked generalization. In *Advances in Neural Information Processing Systems*.
- [124] Johannes Zagermann, Ulrike Pfeil, and Harald Reiterer. 2016. Measuring cognitive load using eye tracking technology in visual computing. In *Proceedings of the sixth workshop on beyond time and errors on novel evaluation methods for visualization*. 78–85.
- [125] Wei-Long Zheng, Bo-Nan Dong, and Bao-Liang Lu. 2014. Multimodal emotion recognition using EEG and eye tracking data. In *2014 36th Annual International Conference of the IEEE Engineering in Medicine and Biology Society*. IEEE, 5040–5043.
- [126] Feng Zhou, Areen Alsaied, Mike Blommer, Reates Curry, Radhakrishnan Swaminathan, Dev Kochhar, Walter Talamonti, Louis Tijerina, and Baiying Lei. 2020. Driver fatigue transition prediction in highly automated driving using physiological features. *Expert Systems with Applications* 147 (2020), 113204.
- [127] Jianlong Zhou, Syed Z Arshad, Simon Luo, Kun Yu, Shlomo Berkovsky, and Fang Chen. 2017. Indexing cognitive load using blood volume pulse features. In *Proceedings of the 2017 CHI Conference Extended Abstracts on Human Factors in Computing Systems*. 2269–2275.
- [128] Zhi-Hua Zhou. 2025. *Ensemble methods: foundations and algorithms*. CRC press.

A Model Hyperparameter Configuration

Table 6 summarises the hyperparameters used for the CatBoost and XGBoost classifiers in the cross subject evaluation. The configurations were selected to provide stable training while limiting overfitting and keeping training time manageable.

B Feature Computation and Statistical Metrics

The ocular and cardiac features were calculated within fixed resampling windows, with corresponding formulas and statistical metrics summarised in Table 7 and Table 8.

Table 6: Model hyperparameters for SVM, CatBoost and XGBoost.

Model	Hyperparameters
Linear SVM	C = 1.0 class_weight = {0: 1.0, 1: float(spw)} random_state = 42
	iterations = 600 depth = 6 learning_rate = 0.05 l2_leaf_reg = 3.0
CatBoost	loss_function = Logloss eval_metric = Logloss verbose = False random_state = 42 class_weights = [1.0, max(1.0, spw)]
	n_estimators = 400 max_depth = 5 learning_rate = 0.05 subsample = 0.8 colsample_bytree = 0.8 min_child_weight = 5 reg_lambda = 1.5 reg_alpha = 0.0 gamma = 0.2 objective = binary:logistic class_weights = [1.0, max(1.0, spw)] tree_method = hist random_state = 42 eval_metric = logloss
XGBoost	n_estimators = 10 max_depth = 2 learning_rate = 0.08 subsample = 1.0 colsample_bytree = 1.0 min_child_weight = 1.0 reg_lambda = 1.0 objective = binary:logistic scale_pos_weight = float(spw) eval_metric = logloss n_jobs = 1 tree_method = hist random_state = 42
XGBoost (Fusion Model)	

C Extracted Features and Final Feature Sets for Ocular and Cardiac Modalities

Table 9 summarises the complete set of ocular and cardiac features extracted from the raw signals, together with the final subset retained for model training. The complete set includes all features produced during preprocessing, whereas the final set contains only the measures retained after eliminating variables with low discriminative power or high collinearity.

Table 7: Description and Statistical Metrics of Eye-Tracking Features.

Eye Feature	Description with Formula	Statistical Metrics
Pupil Diameter	Pupil diameter calculated separately for left, right, and both eyes within the resampling window.	Mean, Min, Max, SD
Saccade Amplitudes	Angular distance of saccades in degrees. Formula: $\theta = 2 \arctan\left(\frac{d}{2D}\right)$, where d is the pixel distance and D is the viewing distance.	Mean, Max
Saccade Velocity	Velocity of saccades in degrees/second. Formula: $v = \frac{\Delta\theta}{\Delta t}$.	Mean, Max
Saccade & Fixation Count	Event counts within each resampling window.	Mean
Saccade & Fixation Rate	Per-second event rate. Formula: Rate = $\frac{\text{Event Count in Window}}{\text{Window Duration (s)}}$.	Rate
Saccade/Fixation Ratio	Ratio of total saccade duration to total fixation duration. Formula: SFR = $\frac{T_{\text{saccade}}}{T_{\text{fixation}}}$.	Ratio
Fixation Duration	Average fixation duration. Formula: $FD = \frac{\sum_{i=1}^N t_i}{N}$, where t_i is each fixation duration and N the number of fixations.	Mean, Max, Sum
Area of Interest (AOI)	AOIs defined from in-game screenshots by HSV colour filtering, edge detection, and contour extraction. Coordinates saved as pixel and normalised values. Portion Formula: AOI Portion = $\frac{\text{Samples in AOI}}{\text{Total Samples}}$. Rate Formula: AOI Rate = $\frac{\text{Entries into AOI}}{\text{Window Duration}}$.	Portion, Rate

Table 8: Description and Statistical Metrics of Cardiovascular Features.

Cardiac Feature	Description with Formula	Statistical Metrics
Heart Rate (HR)	Number of heartbeats per window. Derived from interbeat intervals (IBIs). Formula: $HR = \frac{60}{\text{IBI}}$, where IBI is in seconds.	Mean
Heart Rate Variability (HRV)	Two indices computed from NN intervals. $\text{RMSSD} = \sqrt{\frac{1}{N-1} \sum_{i=1}^{N-1} (NN_{i+1} - NN_i)^2}$ $\text{MeanNN} = \frac{1}{N} \sum_{i=1}^N NN_i$	Mean
Blood Volume Pulse (BVP) Statistics	Signal statistics across a window. Mean: $\mu = \frac{1}{N} \sum_{i=1}^N x_i$ Std: $\sigma = \sqrt{\frac{1}{N} \sum_{i=1}^N (x_i - \mu)^2}$	Mean, Std

D Areas of Interest for Gaze Features

Table 10 documents the areas of interest (AOIs) used for gaze feature extraction in *Slay the Spire*. Figure 15 illustrates the annotated interface, and the table summarises each AOI element with its function and screen position. These materials provide a transparent basis for how gaze allocation features, such as fixation proportion and dwell time, were derived.

E Feature Importance Results

Table 11 summarises the mean CatBoost feature importance across LOSO folds for the ocular modality, and Table 12 summarises the

mean XGBoost feature importance across LOSO folds for the cardiac modality.

Table 9: Complete extracted feature set and final features used for each modality.

Modality	Complete Extracted Feature Set	Final Features Used
Ocular	Pupil: Left/Right/Avg diameter (Mean, Std, Min, Max); Saccade: Count mean; Rate; Amplitude (Mean, Max); Velocity max; Saccade to fixation ratio; Fixation: Duration (Max, Mean, Sum); AOI: Hand cards (Proportion, Rate); Top bar potion (Proportion, Rate)	Saccade: Count mean; Rate; Amplitude (Mean, Max); Velocity max; Saccade to fixation ratio; AOI: Hand cards (Proportion, Rate); Top bar potion (Proportion, Rate)
Cardiac	BVP Stats: Min; Max; Mean; Std; Variance; RMS; Skewness; Kurtosis; HRV: Mean NN; RMSSD; pNN50; pNN20; Ratio	Heart Rate: Mean Heart Rate; Heart Rate Range

Table 10: Key interface elements in *Slay the Spire* with their positions and functions.

Element	Function / Effect	Typical On-Screen Position
Relics	Permanent passive bonuses that affect the run (e.g., extra energy, healing, card draw).	Top-left area of the screen
Potions	One-time use consumable items used during combat to grant effects (e.g., heal, buff, damage).	Top-middle of the combat interface, in potion slots
Hand Cards	The cards the player currently can play, showing available actions (Attacks, Skills, Powers).	Bottom centre of the screen
Enemy Tooltip	Shows what the enemy intends to do next (e.g., attack amount, defense, buffs/debuffs), guiding player strategy.	Above the enemy on the combat screen

Table 11: CatBoost feature importance for the ocular modality (mean across LOSO folds).

Feature	Importance
Potion bar (AOI proportion)	45.99
Potion bar (AOI rate)	40.88
Hand cards (AOI proportion)	4.29
Hand cards (AOI rate)	3.49
Saccade-fixation ratio	2.36
Saccade rate	1.51
Mean saccade amplitude (deg)	0.54
Max saccade amplitude (deg)	0.40
Max saccade velocity	0.36
Mean saccade count	0.18

Table 12: XGBoost feature importance for the Cardiac modality (mean across LOSO folds).

Feature	Importance
HR Range	0.56
Mean Heart Rate	0.44

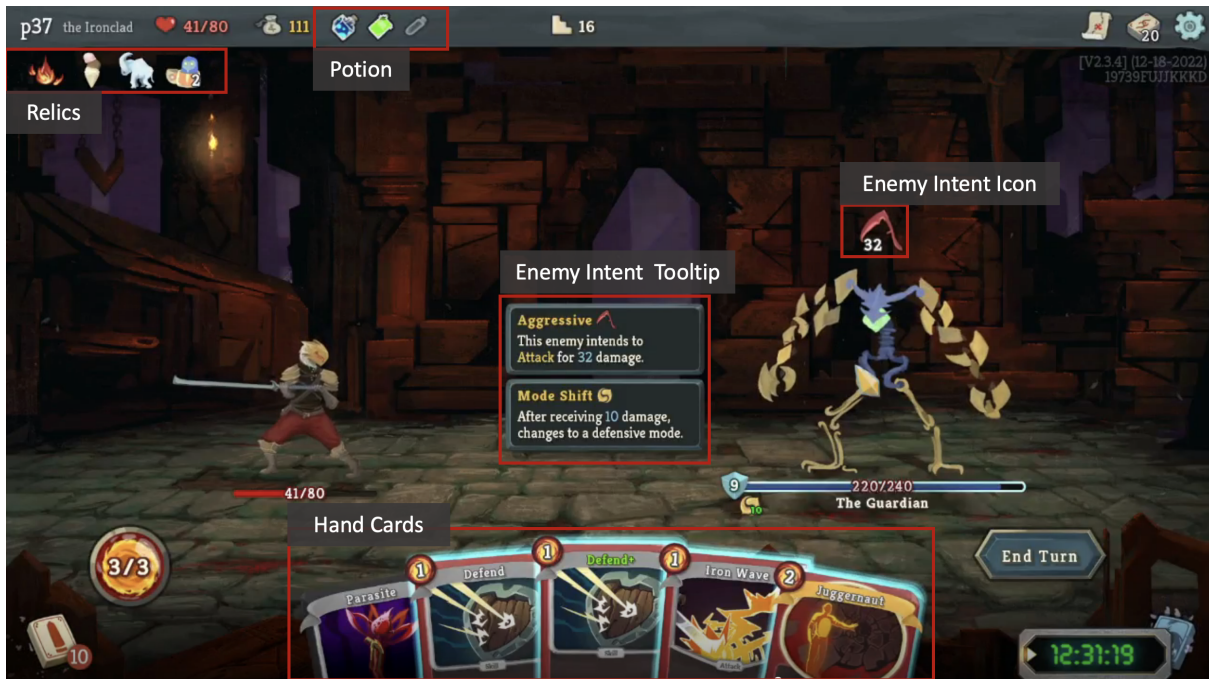


Figure 15: Areas of interest (AOIs) defined for gaze feature extraction in *Slay the Spire*. AOIs included (1) hand cards at the bottom centre (decision options), (2) relics at the top-left (passive bonuses), (3) potions at the top (consumable items), and (4) enemy intent indicators above the opponent, including both the icon and tooltip (upcoming enemy action). These regions provided the basis for deriving gaze features such as fixation proportion and dwell time.